TITANIUM INTERLAYER THICKNESS ON ADHESION OF TiCN THIN FILMS

INFLUENCE OF TITANIUM INTERLAYER THICKNESS ON THE ADHESION OF TiCN THIN FILMS DEPOSITED ON STAINLESS STEEL

By

AUSTIN MICHAEL BROWN, B.Eng.

A Thesis Submitted to the School of Graduate Studies in Partial Fulfilment of the Requirements for the Degree Master of Applied Science

McMaster University

MASTER OF APPLIED SCIENCE (2017), Department of Engineering Physics

McMaster University, Hamilton, Ontario, Canada

TITLE: Influence of Titanium Interlayer Thickness on the Adhesion of TiCN Thin Films Deposited on Stainless Steel

AUTHOR: Austin Michael Brown, B.Eng. (McMaster University)

SUPERVISOR: Professor Peter Mascher

NUMBER OF PAGES: xii, 63

Abstract

Hard coatings deposited by physical vapour deposition (PVD) are commonly used to improve the scratch resistance and hardness of objects made of softer materials such as steel, and they can also be used as decorative coatings since they exhibit a wide range of different colours. In this research, stainless steel tableware utensils were coated with multilayer Ti/TiCN thin films to give the tableware a wear-resistant decorative finish. A cathodic arc PVD system was used to deposit the coatings since it has the potential to produce very dense coatings with excellent adhesion and wear-resistance properties in relatively short deposition times. Several system parameters were varied between deposition cycles to create a large set of samples which included: changing the amount of flatware present inside of the chamber during deposition, changing the size of the flatware used, changing the mounting location of the flatware inside of the chamber, and changing the depletion level of the titanium cathode targets used to deposit titanium. It was found that changing these variables had an effect on the deposition rate of the coating and thus had an effect on the thickness of the titanium interlayer, which was found to be an important factor in achieving good adhesion of the TiCN layer. The optimal titanium interlayer thickness was found to be in the range of approximately 120 to 230 nm.

Acknowledgements

I would first like to thank my parents, Michael and Maureen, for helping me along my academic journey and giving me the encouragement and support that I needed to achieve my goals; I could not have done this without them. I would also like to thank the many friends, family members, and teachers that I have had throughout the years that have also helped me to grow both personally and intellectually on my journey.

I would like to give many thanks and express my great appreciation towards my supervisor, Dr. Peter Mascher, for giving me the opportunity to join his research team several years ago when I was just an undergrad student in second year. While working with him and his students over the last few summers and as a grad student, I have learned so much about vacuum coating and thin film technology and I could not have asked for a better education. Peter has been very supportive over the years in providing me with many different opportunities for success and has continually allowed me to pursue projects that personally interest me. I feel very fortunate to have been a part of his research team during my time here at McMaster.

Special thanks go to Dr. Jacek Wojcik for the hands-on teaching approach that he has given me during his final years in our research group. I consider him to be a great mentor and role model of mine and there has not been another person that has taught and prepared me more for starting a career in the vacuum coating industry than he has.

I would like to thank Dr. John Luxat for allowing me to use the new SEM in the Tandem Accelerator Building and Dr. Zhilin Peng for his continuous support in helping me obtain SEM images for my research. Zhilin was under no obligation to help me but was always willing to let me use his time and resources. I would also like to thank Dr. Ludvik Martinu, Dr. Jolanta Sapieha, and Dr. Thomas Schmitt from the Functional Coating and Surface Engineering Laboratory (FCSEL) at L'École Polytechnique de Montréal for allowing me to use their fantastic tribology lab to analyze my samples, while providing me with valuable advice on potential improvements that I could make towards my research.

Finally, I would like to thank the Natural Sciences and Engineering Research Council of Canada (NSERC) for providing funding for this research through the NSERC Engage program, as well as the Society of Vacuum Coaters (SVC) for providing me with a student scholarship and allowing me to present my research at the 59th Annual SVC TechCon in Indianapolis in 2016.

Publications & Presentations

- A. Brown, S. A. Lyda, J. Wojcik, and P. Mascher, “Application of Titanium Nitride Coatings on Stainless Steel Tableware for Decorative and Protective Purposes,” in *Society of Vacuum Coaters 59th Annual Technical Conference Procedings*, 2016.

- A. Brown, "Application of Titanium Nitride Coatings on Stainless Steel Tableware for Decorative and Protective Purposes", 59th Annual SVC TechCon Student Presentation, Indiana Convention Center, Indianapolis, Indiana, United States, 2016.

Table of Contents

List of Figures

List of Tables

List of Abbreviations & Symbols

CVD	Chemical Vapour Deposition
FIB	Focussed Ion Beam
L_{C1}	Critical Load 1
L_{C2}	Critical Load 2
L_{C3}	Critical Load 3
PACVD	Plasma Assisted Chemical Vapour Deposition
PECVD	Plasma Enhanced Chemical Vapour Deposition
PLD	Pulsed Laser Deposition
PVD	Physical Vapour Deposition
SCCM	Standard Cubic Centimeter per Minute
SEM	Scanning Electron Microscope
TiCN	Titanium Carbo-Nitride
TiN	Titanium Nitride
σ	Standard Deviation

Declaration of Academic Achievement

This dissertation is the result of my own work and includes nothing which is the outcome of work done in collaboration except where specifically indicated in the text. I declare that I have composed the presented paper independently on my own and without any other resources than the ones indicated. All thoughts taken directly or indirectly from external sources are properly denoted as such. This dissertation has not been previously submitted, in part or whole, to any university or institution for any degree, diploma, or other qualification.

Austin Michael Brown
McMaster University

Introduction

Hard Titanium Ceramic Coatings

Hard coatings deposited by physical vapour deposition (PVD) and chemical vapour deposition (CVD) are seeing widespread use in many industries due to their desirable mechanical and decorative properties. Titanium-based ceramic coatings such as TiN and TiCN are commonly deposited on machine parts such as drill bits and cutting tools to enhance their surfaces, providing them with substantially greater corrosion and wear resistance than uncoated steel. These coatings are also well suited for use as decorative coatings since TiN has a distinct gold colour and TiCN can vary from bronze to violet depending on the carbon content of the film. These coatings are also much more durable than decorative coatings produced using other techniques such as electroplating gold and copper [1].

TiN and TiCN coatings are most commonly deposited by PVD techniques such as magnetron sputtering, cathodic arc deposition, and pulsed laser deposition (PLD) [2]. These deposition techniques all involve ejecting particles of titanium from pure solid sources of titanium, commonly referred to as targets, by imparting energy to the targets using ions, electrons, and photons respectively. Alternatively, chemical vapour deposition (CVD) can be used to obtain titanium ceramic coatings. CVD utilizes gaseous

chemical precursors containing titanium (most commonly titanium tetrachloride [3]), rather than solid titanium targets, whereby the precursor gases react and decompose inside of the vacuum chamber, releasing titanium atoms which then can deposit on the surface of the substrate to form a thin film [2]. There are a number of ways in which the titanium atom can be released from the precursor gas molecule which is what distinguishes each CVD method from one another. Plasma enhanced and plasma assisted chemical vapour deposition (PECVD and PACVD respectively), as well as thermal chemical vapour deposition, are the most common techniques used to deposit titanium-based ceramic thin film coatings [2]. The biggest advantage of using CVD over PVD is that it is not a line-of-sight process, enabling CVD to evenly coat complex geometries that cannot be achieved by PVD [2], [3], [4]. One of the disadvantages of CVD however, is that the process by-products are quite toxic due to the volatile nature of the precursor gases, whereas PVD techniques do not produce harmful by-products [2].

If depositing TiN or TiCN on steel tools, thermal CVD is typically an unfeasible deposition method since the high deposition temperatures required to break the precursor gas bonds (~1000 ˚C) are in the same range that is used in the initial heat treatment of many tool steels. Post-treatment hardening and tempering may be required after deposition to re-harden the steel substrate which may compromise the dimensional tolerances of the tool as well as the adhesion quality. For depositing CVD hard coatings

on steel, PACVD and PECVD should strictly be used which can break the precursor gas bonds at much lower chamber temperatures due to the added energy from the plasma [3].

Both TiN and TiCN deposited by either PVD or CVD typically form crystals in the NaCl (B1) structure [2], [5]. Titanium ceramic coatings deposited by PVD methods however, are characterized by columnar grains that are elongated along the growth direction, with lengths typically spanning the entire thickness of the coating. For CVD processes, the initial grain sizes of titanium ceramic coatings are very fine, after which a preferred orientation forms followed by the formation of elongated grains in the direction of growth [3]. Regardless, both PVD and CVD can produce titanium ceramic coatings with exceptional wear resistance and adhesion properties [2].

In this research, type 304 stainless steel flatware utensils such as forks and spoons were coated with multilayer thin films of Ti/TiCN using a large commercial cathodic arc PVD system to give them a coloured appearance resembling that of rose gold or copper. This research focuses on improving the adhesion of the Ti/TiCN multilayer coating on the stainless steel substrate by investigating several deposition parameters including the amount of flatware present inside of the chamber during deposition, the size of the flatware used, the location of the flatware inside of the chamber, and the level of depletion of the titanium cathode targets. These variables all have an effect on the deposition rate of the coating and thus have an effect on the thickness of the titanium

interlayer (or 'glue layer') which has been suggested in literature to be of critical importance in achieving good adhesion of the TiCN coating [6].

TiCN is an excellent thin film material to use for improving the wear-resistance of soft metals as it is approximately 20 times harder than stainless steel. In the research conducted by Randhawa [7], microhardness tests using a Knoop indenter were performed on TiCN thin films that were prepared by varying the material composition of the film and the deposition temperature. All of the TiCN thin films that were deposited had thicknesses between 5 and 7 μm, and the results of the microhardness tests can be found in Table 1.

Table 1: Microhardness variations in TiC_xN_{1-x} thin films versus substrate temperature [7].

Composition	*Microhardness (kgf·mm^{-2}) at the following deposition temperatures*		
	400 ˚C	*500 ˚C*	*600 ˚C*
TiN	2550	2600	2650
$TiC_{20}N_{80}$	2650	2600	2600
$TiC_{30}N_{70}$	2700	2650	2500
$TiC_{50}N_{50}$	2850	2700	2650
TiC	3000	3300	3700

Considering that the Knoop microhardness of type 304 stainless steel is only 138 kgf·mm^{-2} [8], it is understandable why hard PVD coatings such as TiCN make high performance wear-resistant coatings. To take advantage of the wear-resistance properties of hard PVD coatings however, film thicknesses typically need to be at least 5 μm as it

has been shown that the wear-rate of TiN thin films can be significantly reduced by increasing film thickness up to 5 μm, and thicknesses beyond 5 μm exhibit only marginal improvements in reducing wear-rate [9], [10], [11]. The thicknesses of the decorative TiCN coatings that were deposited for the research found in this dissertation are all less than 1 μm, providing only minimal improvements in wear-resistance compared to the uncoated stainless steel surface. For decorative coating applications, the appearance of the coating is the primary concern, namely colour and texture, and the superior wear-resistance that a thicker coating can provide is largely unnecessary. Increasing coating thickness means increasing deposition duration, which results in an unnecessary increase in production costs.

Cathodic Arc Deposition

Cathodic arc deposition utilizes high-current/low-voltage electrical arcs between an anode and cathode to vaporize the cathode material so that it can be deposited as a thin film. Taking place inside of a vacuum chamber, the arc is initiated by touching the anode to the cathode using a linear actuator such as a solenoid, and then separating them by a small distance. After the electrodes are separated, the electrical arc is conducted from the anode to the cathode through the ejected vapour of the cathode material, and a plasma of the cathode material forms between the two electrodes [12]. The areal power density

associated with the arc spot on the cathode surface is approximately 10^9 W/cm^2, which is sufficiently large to transform the solid cathode material into the plasma phase in a very short time period of only 10 to 100 ns [13]. The high power densities of the cathode spots ensure that the ejected plasma of the cathode material is nearly 100% ionized and often contains multiply charged ions [12], [13].

In this research, cathodic arcs were used with a current of approximately 100 A and a voltage of approximately 20 V. The voltage only needs to be sufficient to overcome the ionization potential of the cathode material to be vapourized [12]. There is a minimum current known as the chopping current that is needed for stable and self-sustained operation of the arc. Arc currents lower than the chopping current will cause the arc to extinguish itself when the power density at the active cathode spot has decreased. Arc currents higher than the chopping current have a high likeliness of igniting new cathode spots when the power density at the active spot drops. The chopping current of the electrical arc is dependent on the cathode material; for pure titanium the chopping current is approximately 50 A [13].

Pure titanium is deposited onto the surface of any object inside of the chamber that is positioned within a line of sight of a titanium cathode target while it is active. To deposit materials such as TiN or TiCN, process gases such as nitrogen and acetylene can be introduced into the chamber to react with the arc plasma in a process called reactive arc deposition. Positively charged ions of arc-ejected titanium and of the process gases

are available in a mixed plasma state to be deposited onto the surface of any object inside of the chamber [14]. To get the ions to react and adhere to the surface of the substrates, a negative bias voltage can be applied to the substrates using a dedicated bias power supply, which causes the positive ions to accelerate towards the substrates. Resistive heaters located on the inner walls of the chamber are used to increase the substrate temperature during pump down and deposition. Heating the substrates to high temperatures under vacuum (i.e. >150 ˚C) will help remove contaminants such as water and weakly-bonded hydrocarbons from the surface of the substrates [15].

Since the reactive coating process is dependent on the gases that are present inside of the chamber during deposition, the chamber must be pumped down to a high vacuum before deposition to ensure that the amount of contaminants in the deposited coating is minimized. In this research, the high vacuum level of the deposition chamber is achieved by using a large diffusion pump. A diffusion pump consists of a cylindrical stainless steel chamber which houses three vertically stacked cones that act as pressure jets for gaseous oil. A diagram of this can be seen in Figure 1.

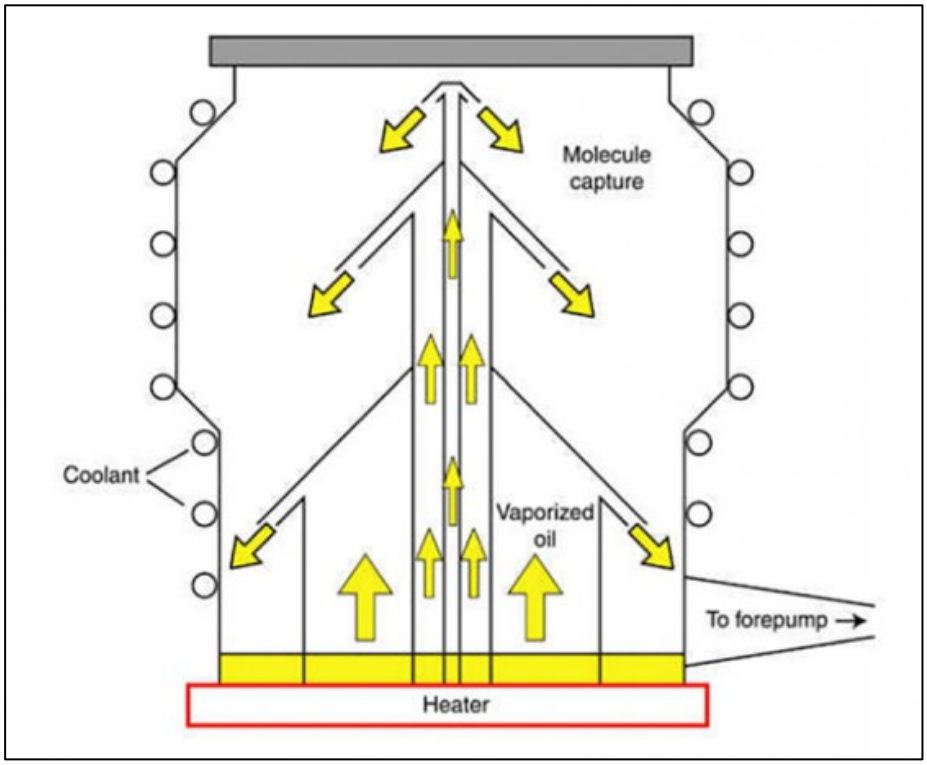

Figure 1: Diagram of diffusion pump operation [16].

Silicone diffusion pump oil is heated at the bottom of the chamber to its boiling point at approximately 215 ˚C [17], whereby it can then travel upwards through the pressure jets before it is directed downward at an angle towards the walls of the diffusion pump chamber. Air inside of the diffusion pump diffuses into the gaseous oil and is brought further down into the diffusion pump chamber. The chamber walls are water-cooled to allow the hot gaseous oil to condense and release the trapped air molecules back into the chamber at a lower position. The released air is now at a higher pressure than it was before it was diffused into the oil, leaving the top of the diffusion pump at a lower pressure than it was previously. A mechanical holding pump is attached near the bottom

of the diffusion pump chamber to pump away the relatively higher pressure air, and the process repeats itself until the desired vacuum level is achieved at the top of the diffusion pump where it is connected to the main deposition chamber [16].

Inside of the deposition chamber, the samples are mounted on racks on a rotating carousel to improve film uniformity. Since the titanium cathode targets are located on the walls of the chamber and eject titanium ions toward the center of the chamber, surfaces that are closer to the center of the chamber will have less titanium deposited on them than surfaces closer to the targets. Rotating the utensils will minimize the difference in coating thickness not only between utensils, but also between different areas on the same utensil. A schematic diagram of the cathodic arc PVD chamber used in this research can be found in Figure 2.

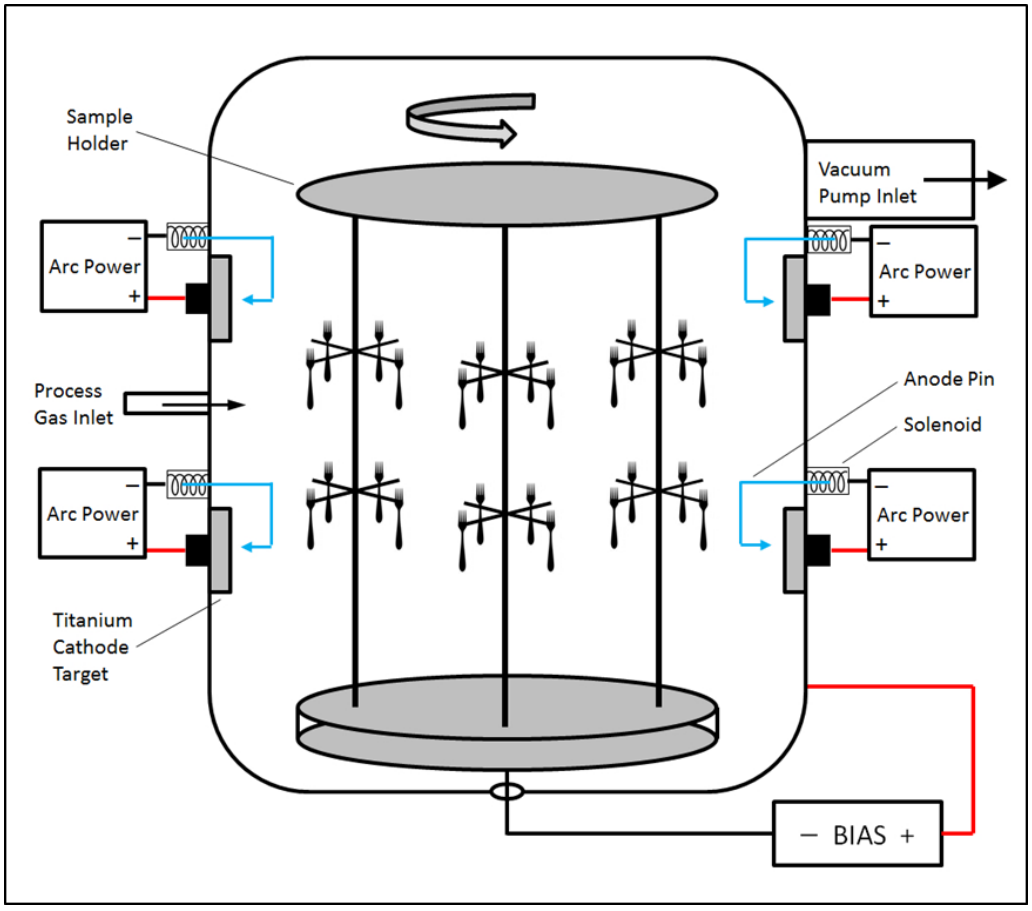

Figure 2: Schematic diagram of a cathodic arc PVD chamber.

The main disadvantage of cathodic arc deposition is the presence of macroparticles in the material that is ejected from the cathode spot. Ideally, the ejected material should consist entirely of positively charged ions, however, large molten globules of the cathode material can be ablated from the surface of the target by thermal shock of the electrical arc. The number and size of the macroparticles produced during cathodic arc deposition depends on several factors including arc current, reactive gas partial pressure, and the melting point of the cathode material [18]. Macroparticles make

cathodic arc deposition an unsuitable deposition method for many technologies such as those found in optics and photovoltaics where film uniformity is essential. For hard mechanical coatings, the presence of macroparticles may or may not be an issue depending on the application. In the application of decorative coatings on mirrored surfaces for example, an increase in the number of macroparticles results in a coating that appears grainier and less reflective, and reducing the macroparticle density in the coating should be a priority to conserve the mirrored finish of the product. Increasing the partial pressures of the reactive gases inside of the chamber during deposition is one way to reduce macroparticle content, as is decreasing the current of the electrical arc at the expense of a lower deposition rate [18].

Another method to reduce the production of macroparticles during deposition is to use curved macroparticle filters attached to all of the cathode targets. When the cathode material is ejected from the target via the electrical arc, the charged ions can be guided electromagnetically through the curved filter tube whereas the neutral macroparticles will travel in straight lines and collide with the walls of the filter instead of depositing onto the substrate. The greater the angle of the bend in the filter, the lower the macroparticle density is in the film, however, larger bends also result in larger losses in the useful plasma and lead to lower deposition rates [13]. A diagram of a typical macroparticle filter can be seen in Figure 3.

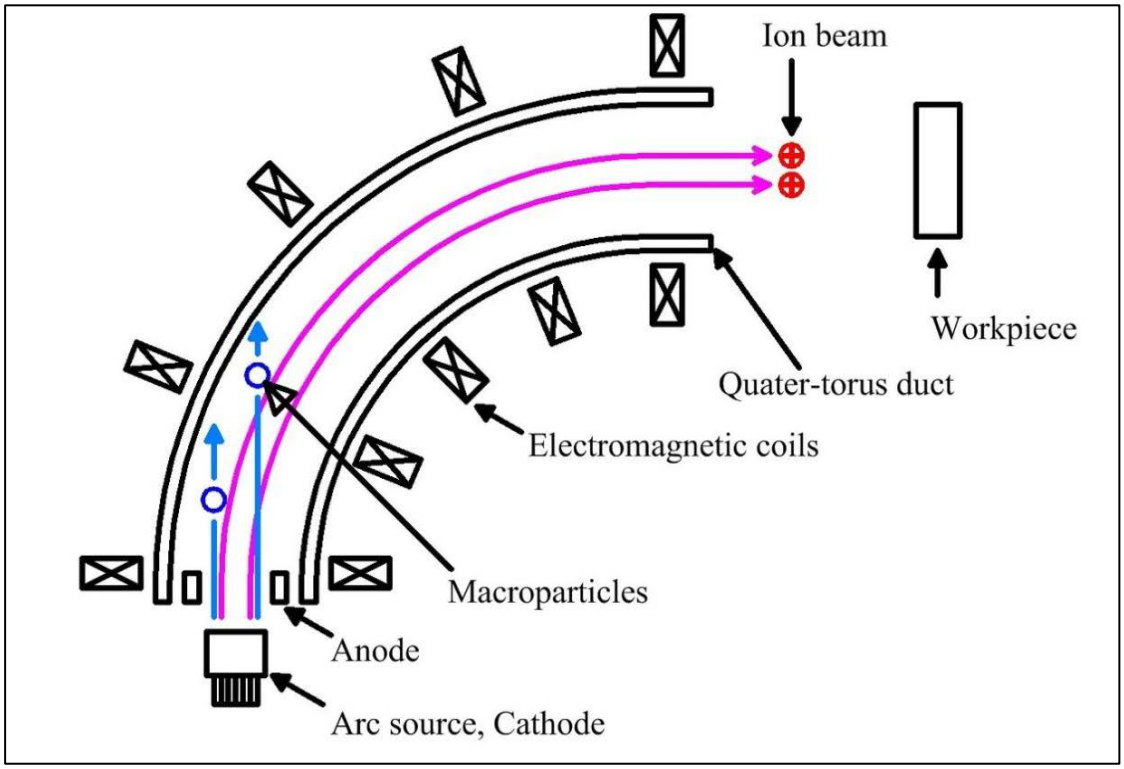

Figure 3: Diagram of a curved macroparticle filter [19].

Nevertheless, cathodic arc deposition is a very effective method for producing hard protective/decorative coatings since cathodic arc plasmas have a very high degree of ionization and the ions ejected from the cathode have very high energies (19 to 150 eV, depending on cathode material). These features give cathodic arc deposition the potential to create highly dense films that have strong adhesion properties [12], [13].

The Titanium Interlayer

All of the coatings that were deposited onto the stainless steel utensils during this research consisted of two layers. A layer of pure titanium was first deposited onto the surface of the stainless steel substrate followed by a second layer of TiCN. It has been shown in other research that depositing an interlayer of titanium onto a steel substrate prior to the deposition of TiN will significantly improve the adhesion of the TiN coating in many PVD processes. A titanium interlayer thickness between 100 and 300 nm is suggested as the optimal range for improving adhesion of the film [6], [20], [21]. The titanium interlayer has the effect of dissolving weak native oxide layers on the surface of the substrate, and also has the effect of reducing the shear stress across the coating-substrate interface due to the relative softness of titanium compared to both TiN and steel [22]. Figure 4 shows how the titanium interlayer has a chemical 'gettering' effect on the residual oxides left on the surface of the substrate to promote better adhesion of a TiN coating. One of the main foci of the research described in this dissertation is to investigate the influence of the Ti interlayer on the adhesion of TiCN films on stainless steel. Since TiN and TiCN are quite similar materials, it is hypothesized that Ti interlayers with thicknesses between 100 and 300 nm will also improve the adhesion of TiCN coatings on stainless steel substrates.

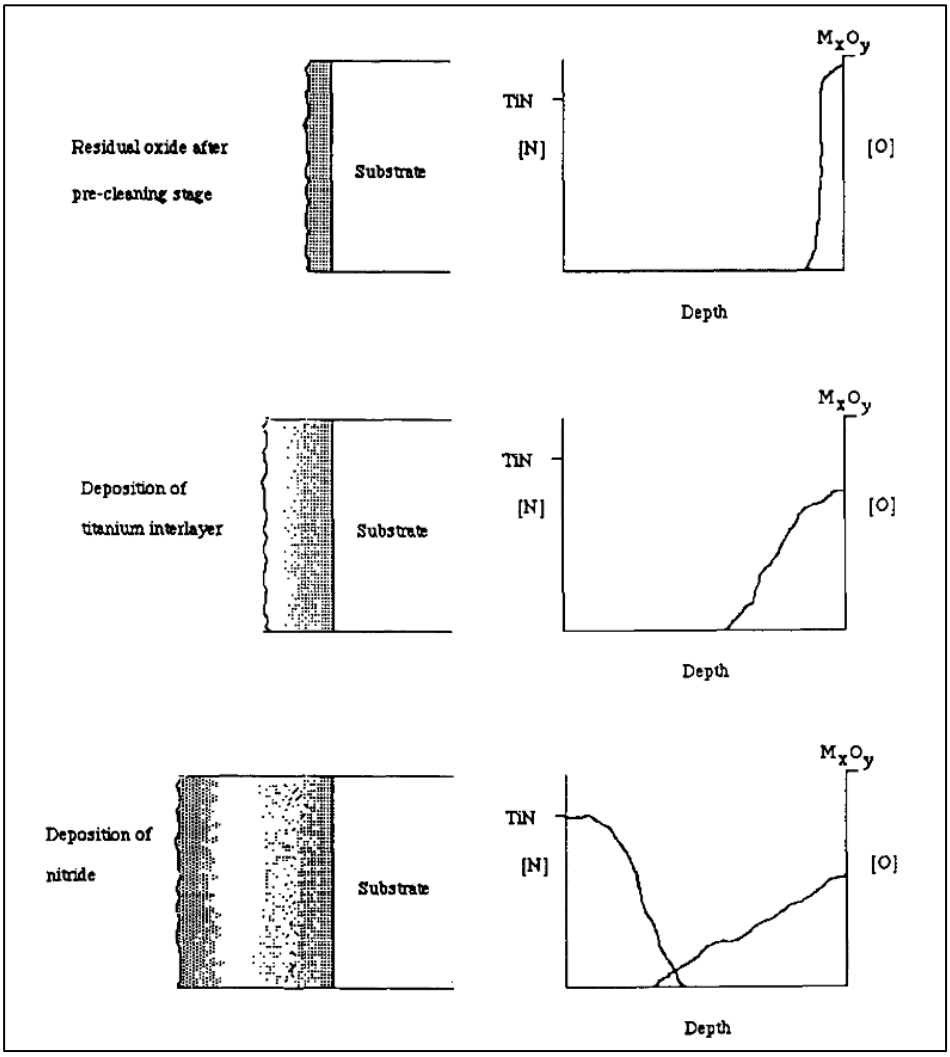

Figure 4: Chemical 'gettering' effect of the titanium interlayer [22].

Experimental Methods

Deposition of the Ti/TiCN Coating

The deposition process sequence that was developed for this research starts with cleaning the uncoated stainless steel utensils. The utensils are first put into an ultrasonic cleaning bath with a degreasing detergent present in the water to remove large particles and oils left over from the utensil manufacturing process. The utensils are then rinsed in clean water, bathed in pure isopropanol, and dried with lint-free cloth before being loaded onto stainless steel mounting racks. Five of these racks, each measuring 42 inches tall and containing up to 96 utensils, are then loaded into the deposition chamber, the chamber heaters are turned on, and the system can begin to pump down.

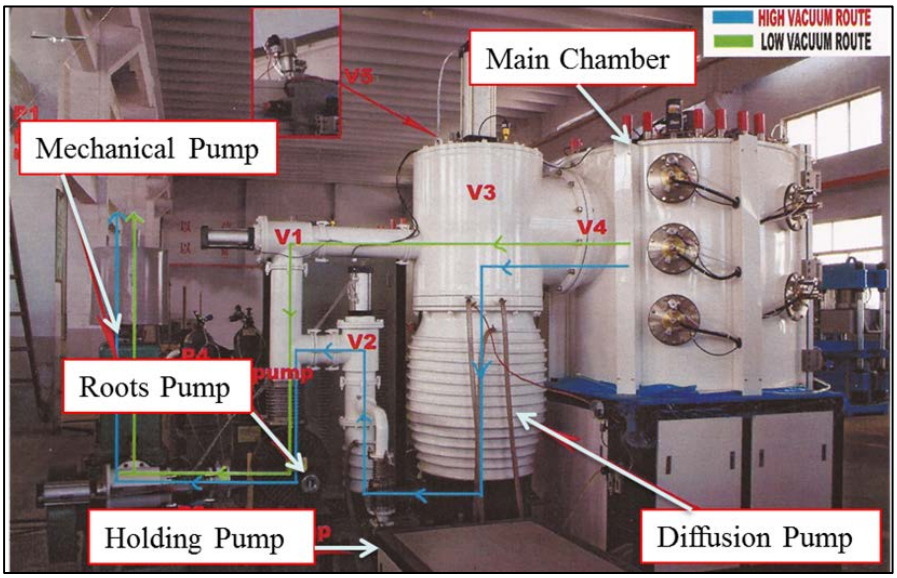

Figure 5: Cathodic arc PVD system used to deposit TiCN coatings in this research.

The pump down process first begins with the mechanical roughing pump, which pumps the system down to 5.5×10^{2} Pa, at which point the roots blower pump is turned on to assist the mechanical roughing pump. This pumping route can be seen as the green path in Figure 5. All vacuum pressures are measured using a Pirani gauge during both the pump down and deposition processes. When the system reaches 3.0×10^{0} Pa, valve V3 opens the diffusion pump to the main chamber. The diffusion pump is backed by a small holding pump before it is opened to the chamber, and when it is opened to the chamber, valve V1 closes and valve V2 opens to allow the large diffusion pump to be backed by the three other pumps. This pumping route can be seen as the blue path in Figure 5. The deposition of the coating can be started once the chamber reaches a base pressure of 7.0×10^{-3} Pa and a temperature of 325 ˚C.

The deposition process begins with a 6 minute argon plasma cleaning step. In this step, argon is introduced into the evacuated vacuum chamber to reach a chamber pressure of 2.0×10^{0} Pa and a very large bias potential of -700 V is applied to the mounting racks and utensils. This large negative bias voltage between the mounting racks and the chamber walls causes the argon to readily ionize into plasma, whereby the positive argon ions in the plasma are accelerated towards the utensils at a high velocity. The acceleration of argon ions onto the surface of the utensil removes any residual contaminants or particles that may have been left on the surface after substrate cleaning, and helps prepare the substrate surface for the deposition of the coating. The energy of

the accelerated argon ions is generally too low to cause surface damage or sputtering of the substrate, but is effective in the desorption of adsorbed surface contaminants such as water [23].

After completing the argon plasma cleaning, a step known as titanium ion implantation or ion bombardment is performed for 1 minute. In this step, electrical arcs are used to evaporate titanium ions from the cathode targets which are then accelerated toward the utensils by applying a bias voltage of -400 V to them. Under the influence of this strong electric field, the Ti ions are imparted with a large amount of kinetic energy and are able to remove more material from the substrate surface than is deposited when the ions collide with the utensils [13]. The high bias voltage also allows Ti ions to be implanted a few nanometers into the surface of the stainless steel substrate, which helps improve the film-substrate interface [24]. Arc-deposited Ti/TiN films that include an ion bombardment step preceding the deposition of the titanium interlayer typically have superior adhesion properties [6]. Previous research has also been conducted using this PVD system that showed that the inclusion of a titanium ion bombardment step in the deposition of Ti/TiN coatings resulted in significant adhesion improvements [25], [26].

The next step is to deposit the titanium interlayer. This layer of pure titanium is deposited by evaporating titanium from the cathode targets and applying a bias voltage of -80 V to the utensils. This lower voltage is necessary to avoid the titanium ions getting implanted into the surface or removing material from the surface, as was the case in the

Ti ion bombardment step. The duration of this step was varied in several of the deposition cycles carried out in this research to see what the effect of different Ti interlayer thicknesses was on the adhesion of the TiCN coating.

The final step of the deposition is to deposit the TiCN coating on top of the Ti interlayer. Acetylene and nitrogen are introduced into the chamber while the Ti cathode targets are evaporated to create a plasma of titanium, carbon, and nitrogen ions. These ions are accelerated towards the utensils by using a substrate bias voltage of -80 V. They then react and condense on the surface of the utensils to create a very dense thin film of TiCN [14]. Since these are primarily decorative coatings, the colour of the TiCN coating is very important to keep within an acceptable range resembling copper or rose gold, which is assessed visually by the operator using a colour palette. Too much acetylene will cause the coating colour to shift towards violet and too much nitrogen will cause the colour to shift towards gold. At different deposition pressures however, the necessary gas flow ratio of nitrogen to acetylene will change in order to produce the desired rose gold colour. A deposition pressure of 4.0×10^{-1} Pa was used to deposit all of the TiCN coatings in this research, and the gas flow ratio that can be used to produce the desired rose gold colour at this pressure is approximately 10:1 nitrogen to acetylene. Typical flow rates that can be used to achieve a pressure of 4.0×10^{-1} Pa in this system while maintaining a 10:1 nitrogen to acetylene gas flow ratio are 400 SCCM of nitrogen and 40 SCCM of acetylene.

Measuring the Titanium Interlayer Thickness

Since a major focus of this research was to determine the influence of the titanium interlayer thickness on the adhesion of the coating, having an accurate method of measuring this thickness was important. Several methods were tested to find the most accurate way of measuring this thickness. The first method that was tested was surface profilometry using devices such as Alpha-Steppers and 3D optical microscopes to measure the height difference between the uncoated substrate and the coating on a partially masked sample. The first problem encountered with this method was that the measured height difference between the masked and unmasked regions of the samples yielded the total thickness of both the Ti interlayer as well as the TiCN layer, which is not particularly useful for this research; rather a method that can independently measure interlayer thickness is much more useful. To try and resolve this, partially masked samples were created this time with different deposition times of the Ti interlayer, without any TiCN layer on top. This is not an ideal representation of the Ti interlayer of the coating since the actual Ti interlayer transitions gradually into the TiCN layer and does not end abruptly as it does in these samples. Furthermore, surface profiling proved to be very challenging with these samples due to the large amount of surface damage and curvature of the stainless steel utensils. For example, the Ti interlayer which is on the order of 100 nm thick is dwarfed by surface imperfections that are several microns high on these utensils.

The second method that was selected to measure the interlayer thickness was using a scanning electron microscope (SEM) equipped with a focussed ion beam (FIB) to view the cross section of the full Ti/TiCN coating on a flat piece of stainless steel. An image of the SEM/FIB system that was used in this research can be seen in Figure 6.

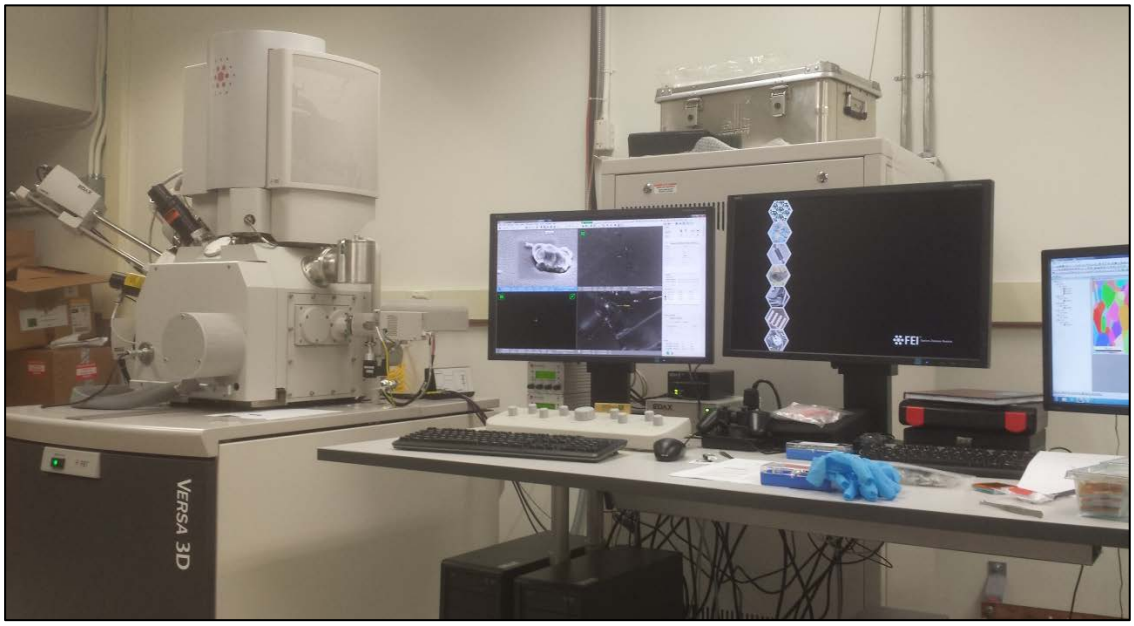

Figure 6: SEM/FIB system used to measure the Ti interlayer thickness.

The SEM uses electric and magnetic fields to accelerate and focus a beam of electrons onto the surface of a sample. This non-destructive interaction generates secondary electrons in the sample which can be detected to provide very high resolution images of the sample in the sub-nanometer range. The FIB operates very similarly to the SEM, however it instead uses electric and magnetic fields to accelerate and focus a beam of ions towards the sample rather than electrons. Ions have significantly more mass than

electrons and when they are accelerated in a FIB, they have enough energy to sputter away the surface of the sample in very precise patterns with nanometer precision [27]. The FIB was used in this research to etch a small area of the sample down to the steel substrate so that the SEM could view the Ti/TiCN multilayer cross section from the side. Although this proved to be more useful at measuring the interlayer thickness than surface profilometry, it was still difficult to see the interface between the steel substrate and the Ti interlayer which added unnecessary experimental uncertainty when trying to estimate where the coating started and ended. An SEM image of a TiCN thin film (~315 nm) on top of a Ti interlayer (~175 nm) deposited on a stainless steel substrate can be seen in Figure 7.

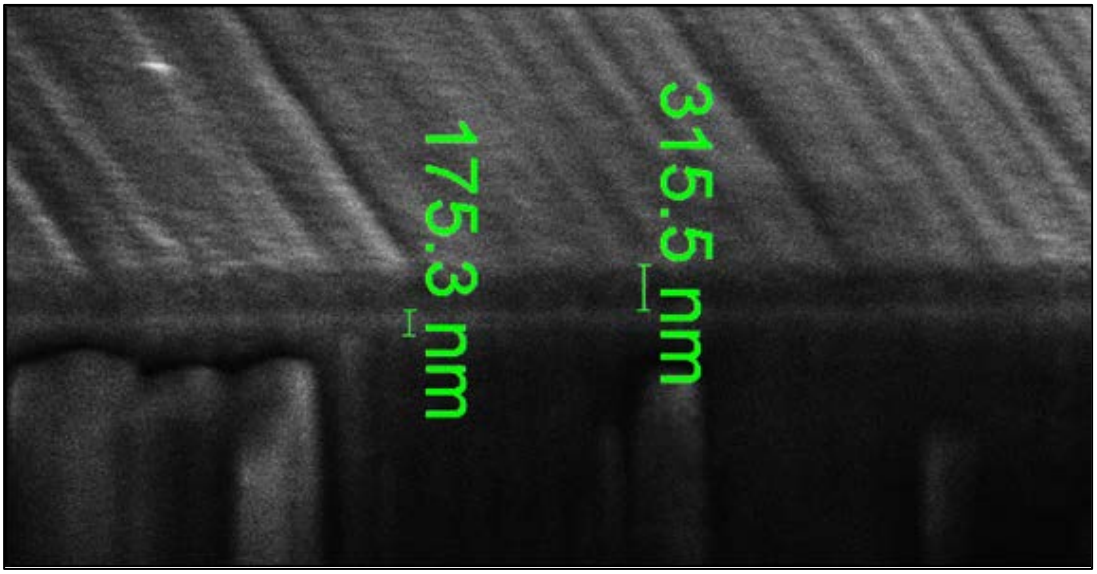

Figure 7: SEM cross section of Ti/TiCN on a stainless steel substrate.

The third method that was tested was to again use the SEM with FIB, but this time with Ti/TiCN coatings that were deposited on silicon wafers instead of stainless steel. Silicon wafers were used in an attempt to improve the SEM images of the substrate/Ti-interlayer interface since they have a much flatter and smoother surface than the stainless steel substrates used in the previous SEM measurements. A silicon wafer was loaded into the deposition chamber along with all of the other stainless steel utensils inside of the chamber so that it could receive the same coating as them. The silicon sample could then be used to accurately determine the Ti interlayer and TiCN film thickness using the SEM/FIB technique, and the stainless steel utensils from that same cycle could be used for adhesion testing. An assumption is made here that the coating thicknesses will be the same on both the silicon and steel substrates when deposited in the same cycle while mounted next to each other. This is a valid assumption since cathodic arc PVD is a line of sight dependent process which is also influenced by the bias potential of the substrate, and the surfaces of both the silicon substrate and the corresponding steel substrate that was used for adhesion testing were mounted very close to one another, oriented in the same direction, and held at the same bias potential. An SEM image of a Ti/TiCN coating on a silicon wafer prepared using this method can be seen in Figure 8 which shows a definite improvement in image quality compared to Figure 7.

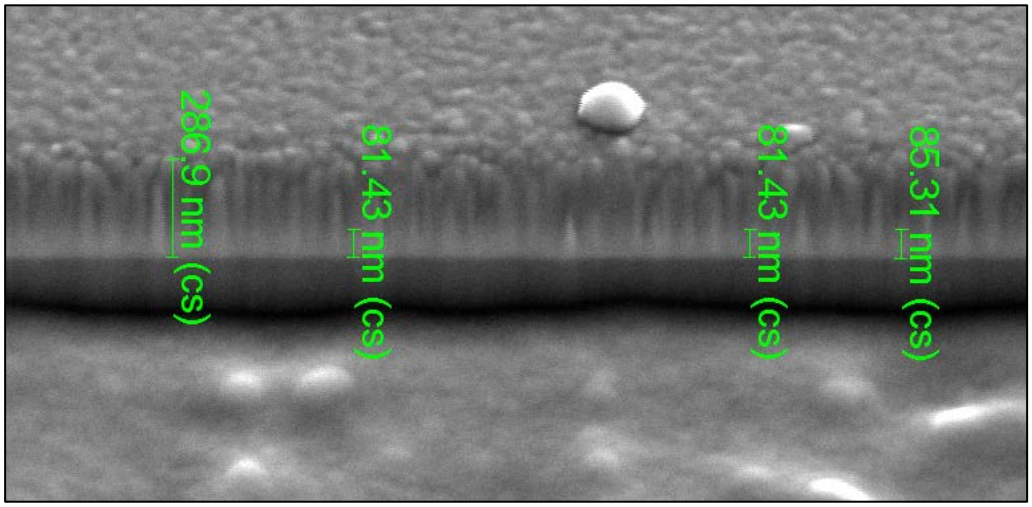

Figure 8: SEM cross section of Ti/TiCN on a silicon substrate.

As can be seen in Figure 8, the interface between the silicon substrate and the Ti interlayer is clearly visible. It is slightly more difficult to see the interface between the Ti and TiCN layers due to the gradual composition change between the two, however by adjusting the contrast levels of the image it is fairly easy to select repeatable criteria for measuring the thickness of the Ti interlayer. An example of this can be seen in Figure 9.

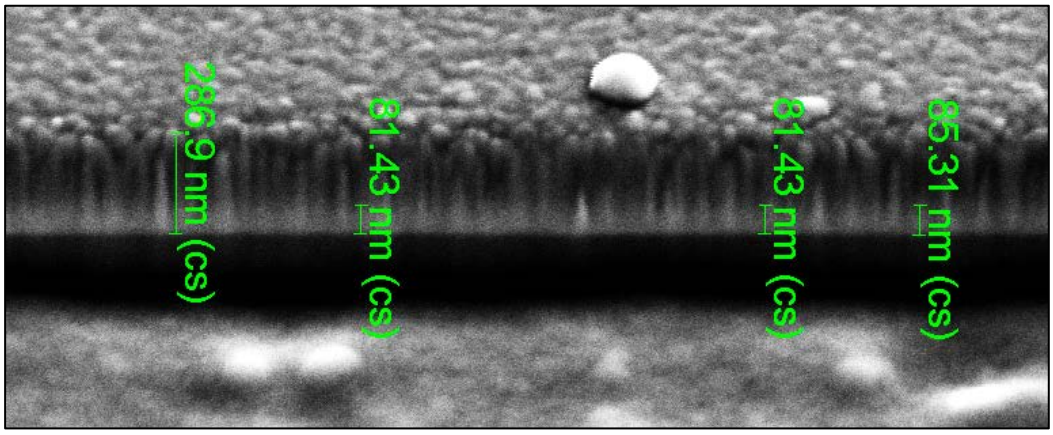

Figure 9: SEM cross section of Ti/TiCN on a silicon substrate with increased contrast.

The digital tool that was used to provide the numerical measurements of the layer thicknesses is built into the SEM software and the results are indicated in green text in all of the SEM images found in this dissertation. Since the cross-section of the film is being looked at from an angle of 52˚ to the normal of the surface of the sample rather than directly at 90˚, it was necessary to use the tool in cross-section mode (denoted by (cs) in the measurement overlay) so that the actual thickness of the layer is indicated to the user instead of the distorted and shortened distance seen in the SEM image as a result of viewing at an angle from above. The measurement tool automatically performs the necessary trigonometric calculations in cross-section mode using the detector angle and the endpoints of the measurement line in the SEM image. One source of uncertainty of the measurement tool was that it required the user to visually select the endpoints of the measurement line which is not perfectly accurate due to the resolutions of the images which were often less than optimal. To address this, several thickness measurements were made on all of the SEM images found in this research using the digital measuring tool and it was consistently found that the measured thicknesses did not vary outside of ± 5 nm of the stated thicknesses presented in this dissertation. All of the thickness measurements in this research therefore have an absolute error of ± 5 nm. This equates to a ± 9% error in the measured thickness of the thinnest sample and only about a ± 1% error in the measured thickness of the thickest sample.

Scratch Testing

Scratch testing was the primary method used to measure the adhesion strength of the TiCN coatings prepared in this research. Scratch testing has been proven to be a simple and reliable method for measuring the relative adhesion quality of coating-substrate systems [28]. A CSM Instruments micro-scratch tester equipped with a Rockwell diamond tip with a radius of 200 μm was used for all of the scratch test measurements found in this dissertation and can be seen in Figure 10.

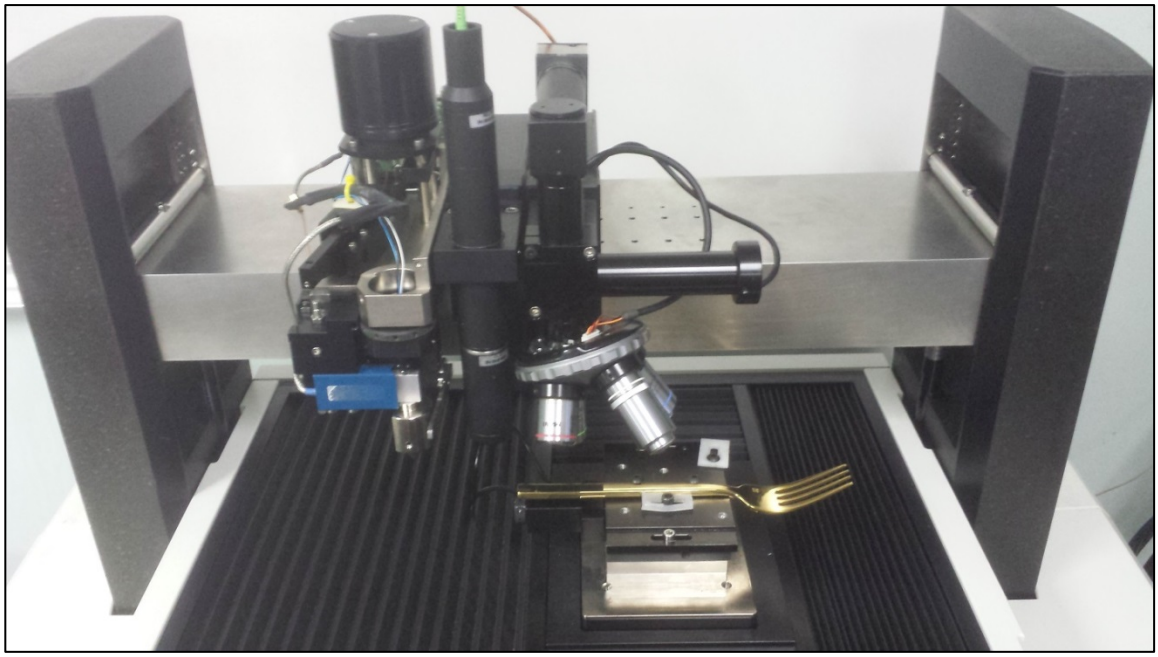

Figure 10: CSM Instruments micro-scratch tester.

The scratches were performed on the coated stainless steel utensils in progressive mode, where the diamond tip travels 6mm along the surface of the sample in a straight

line while the applied load is increased linearly with displacement from 0 to 30 N. Five scratch tests were performed on each sample in five different locations on the sample to acquire statistically justifiable data, and the uncertainty associated with the adhesion values reported in this dissertation are given as the standard error (i.e. $\sigma/\sqrt{5}$) of the five scratch test measurements. Each scratch was examined under an optical microscope to record the force at which the first sign of delamination occurred, the force at which approximately 50% of the coating had delaminated, and finally, the force at which full delamination occurs (>80% delamination). These force measurements are respectively defined as the critical loads L_{C1}, L_{C2}, and L_{C3}, and characterize the adhesion strength of the coating. Examples of the critical load criteria can be seen in Figure 11. Determining the criteria for a critical load is ultimately a subjective choice made by the experimenter, however, consistent use of the critical load criteria between scratches will quantitatively show any relative improvements in adhesion quality [28].

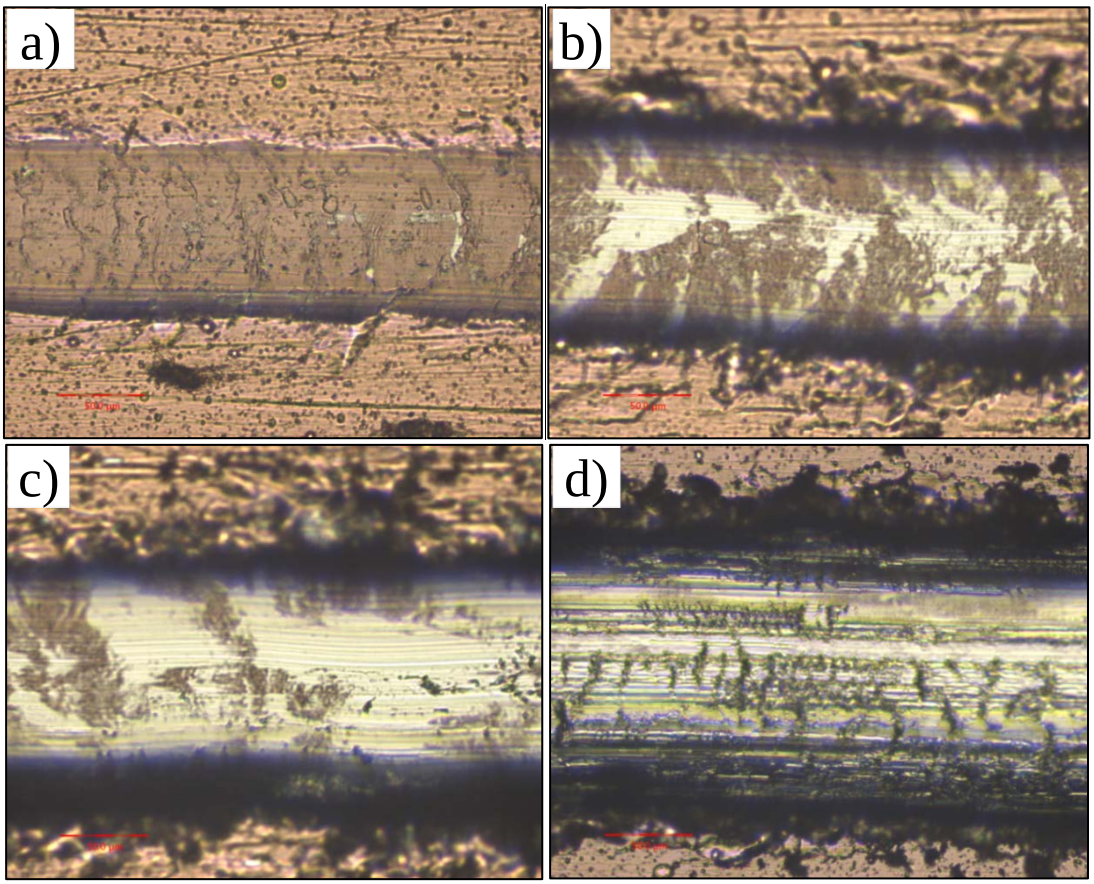

Figure 11: a) An example of L_{C1} where the first instance of delamination occurs, b) an example of L_{C2} where approximately 50% of the coating has delaminated, c) an example of L_{C3} where full delamination has occurred (>80% delamination), and d) another example of L_{C3} where full delamination has occurred (>80% delamination).

Results & Discussion

Ti Interlayer Thickness and Adhesion vs. Deposition Duration

The first experiment that was conducted involved producing and testing three samples that had Ti interlayers deposited for different durations. This would establish a baseline deposition rate for the system using typical deposition parameters before the parameters were varied in subsequent experiments. Adhesion measurements using the scratch testing method were also performed on these samples to see what effect the thickness of the Ti interlayer had on the adhesion of the TiCN coatings. Sample A1 had a Ti interlayer that was deposited for a duration of 3 minutes, Sample A2 had a Ti interlayer that was deposited for a duration of 2 minutes, and Sample A6 had a Ti interlayer that was deposited for a duration of 5 minutes. All 3 samples were fabricated on the same day using the same deposition parameters, other than the duration of the Ti interlayer deposition (i.e. 360 teaspoons inside of the chamber, chamber temperature of 325 ˚C, nitrogen to acetylene ratio of 10:1, deposition pressure of 4.0×10^{-1} Pa, etc.)

Immediately upon taking the utensils out of the chamber after the deposition of sample A2, it was obvious that the adhesion quality was very poor. The majority of the utensils coated during this cycle experienced full delamination failure without any

externally applied stress; they simply came out of the chamber with incomplete coatings, as can be seen in Figure 12. This was not the case with the other samples.

Figure 12: Adhesion failure on sample A2.

Sample A2 had the shortest Ti interlayer deposition duration of all of the samples produced in this research at only 2 minutes, indicating that the thickness of the Ti layer is a crucial factor in the adhesion properties of the TiCN coating. Figures 13, 14, and 15 show SEM cross sections of the Ti/TiCN coatings that were deposited on silicon wafers located beside their respective utensil samples A1, A2, and A6 during each deposition. Sample A2 only has a Ti interlayer thickness of approximately 63 nm which is clearly too thin to facilitate good adhesion.

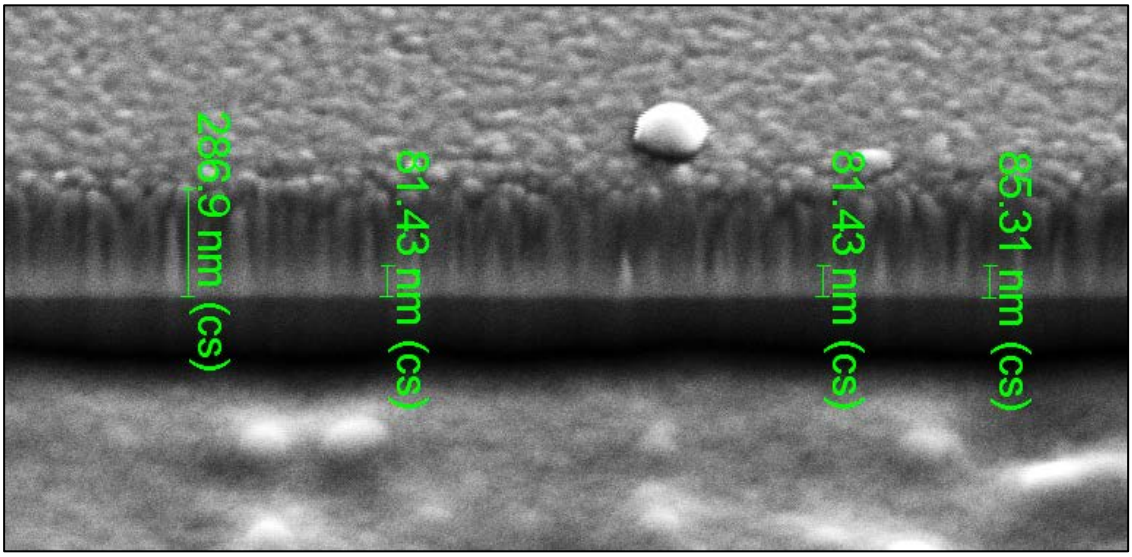

Figure 13: SEM image of sample A1 (Ti interlayer thickness of 83 ± 5 nm).

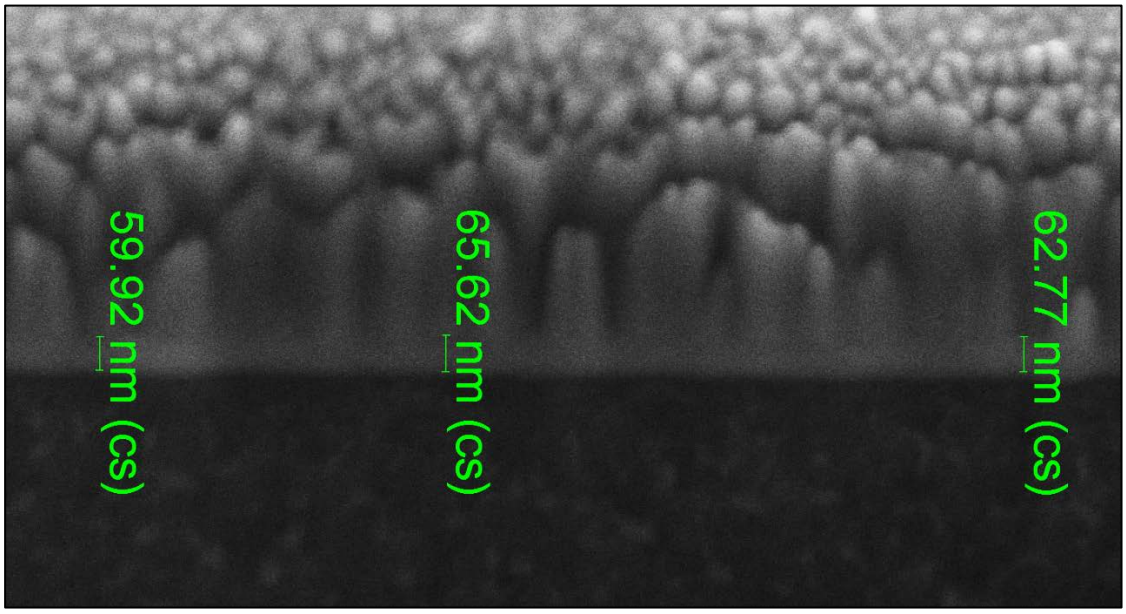

Figure 14: SEM image of sample A2 (Ti interlayer thickness of 63 ± 5 nm).

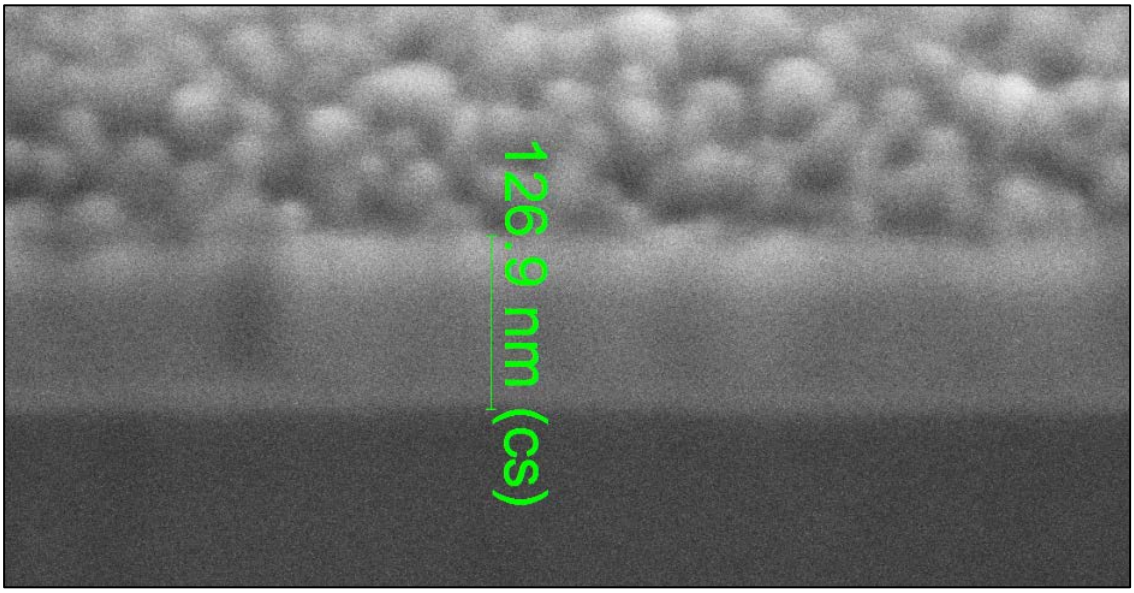

Figure 15: SEM image of sample A6 (Ti interlayer thickness of 127 ± 5 nm).

From these SEM thickness measurements, the deposition rates for each of the titanium interlayers can be calculated and averaged to give an average deposition rate of 28 ± 2 nm per minute. Figure 16 shows a comparison of the adhesion properties of samples A1, A2, and A6 obtained from scratch testing. Since the critical load criteria (i.e. L_{C1}, L_{C2}, and L_{C3}) were met with no applied external force for sample A2, they are indicated simply as 0 N in Figure 16.

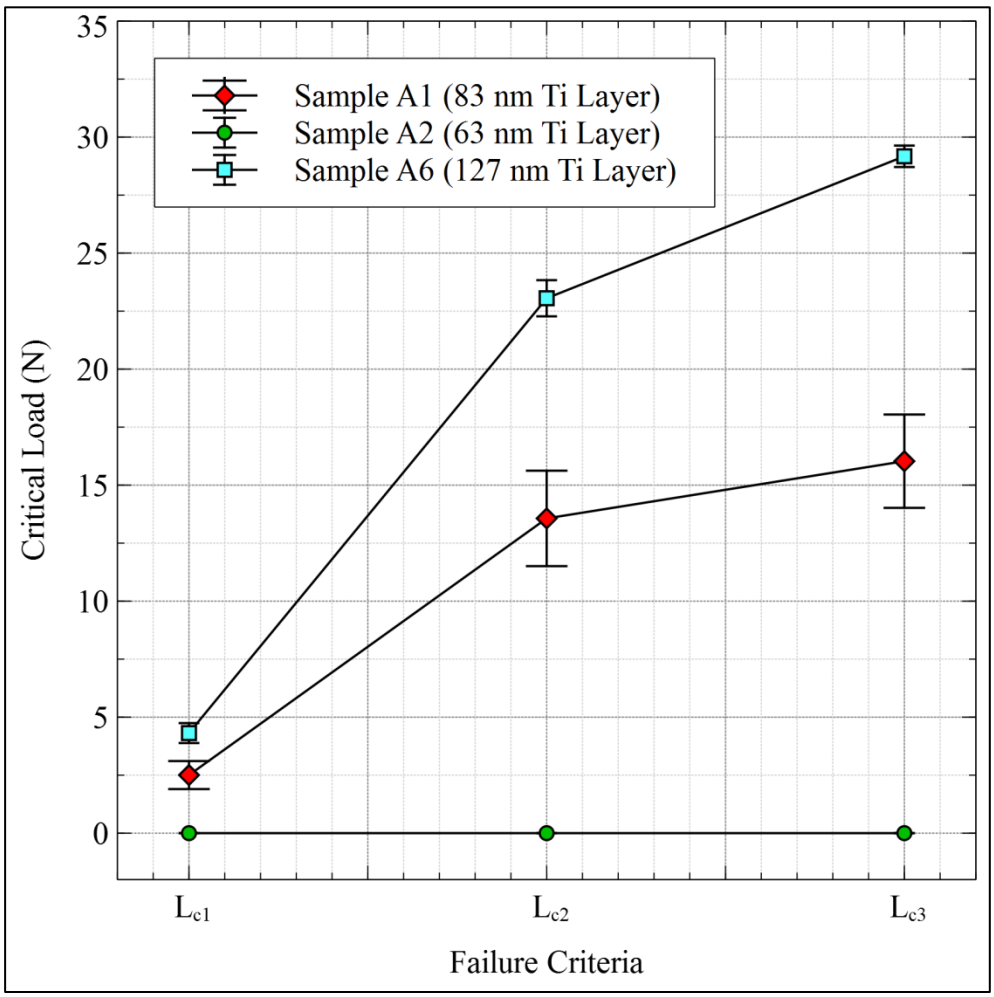

Figure 16: Adhesion results of samples A1, A2, and A6 obtained from scratch testing.

From the scratch test results of these first 3 samples, it is clear that increasing the titanium interlayer thickness to at least 127 nm by increasing the titanium interlayer deposition duration will dramatically improve the adhesion strength of the coating.

Deposition Rate and Adhesion vs. Number of Utensils in the Chamber

Since the cathodic arc deposition chamber is large enough to coat hundreds of pieces of flatware in a single cycle, it is important to understand the influence that the number of pieces inside of the chamber has on the deposition rate of the cycle. Samples A5 and A8 were created in two separate deposition cycles on the same day. Sample A5 was fabricated in a chamber containing only 240 pieces of flatware while sample A8 was fabricated in a chamber containing 480 pieces of flatware. Both cycles had identical deposition parameters with 6 minute Ti interlayers and 9 minute TiCN top layers. SEM images of the two coatings along with their thicknesses can be seen in Figures 17 and 18.

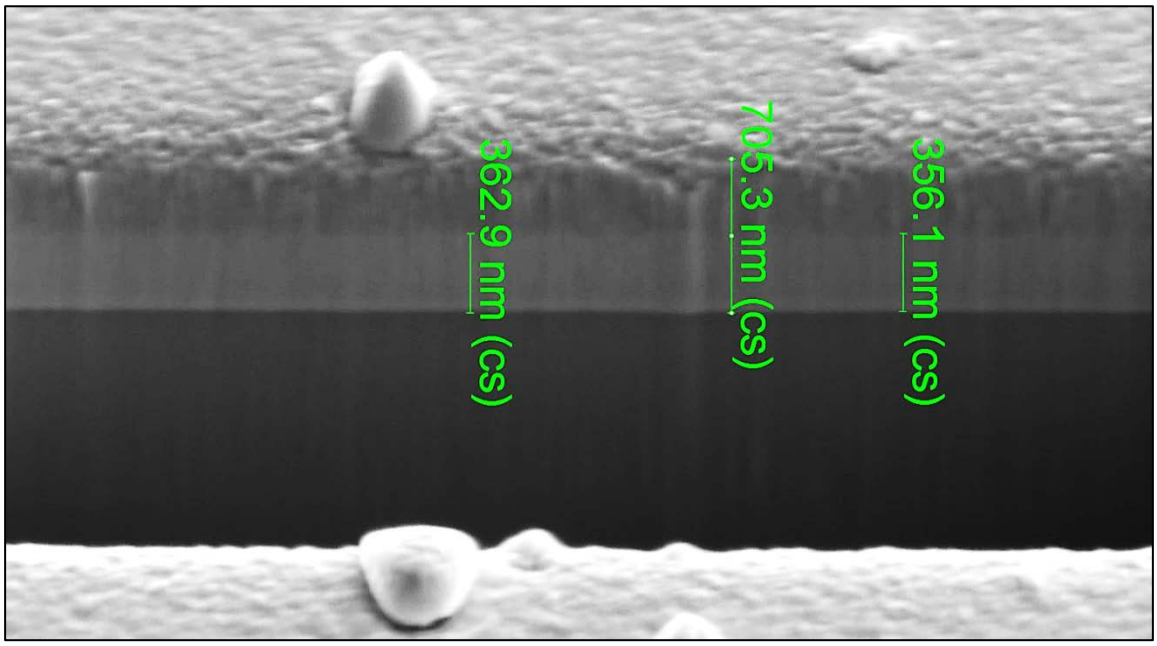

Figure 17: SEM image of sample A5 (Ti interlayer thickness of 360 ± 5 nm, total coating thickness of 705 ± 5 nm).

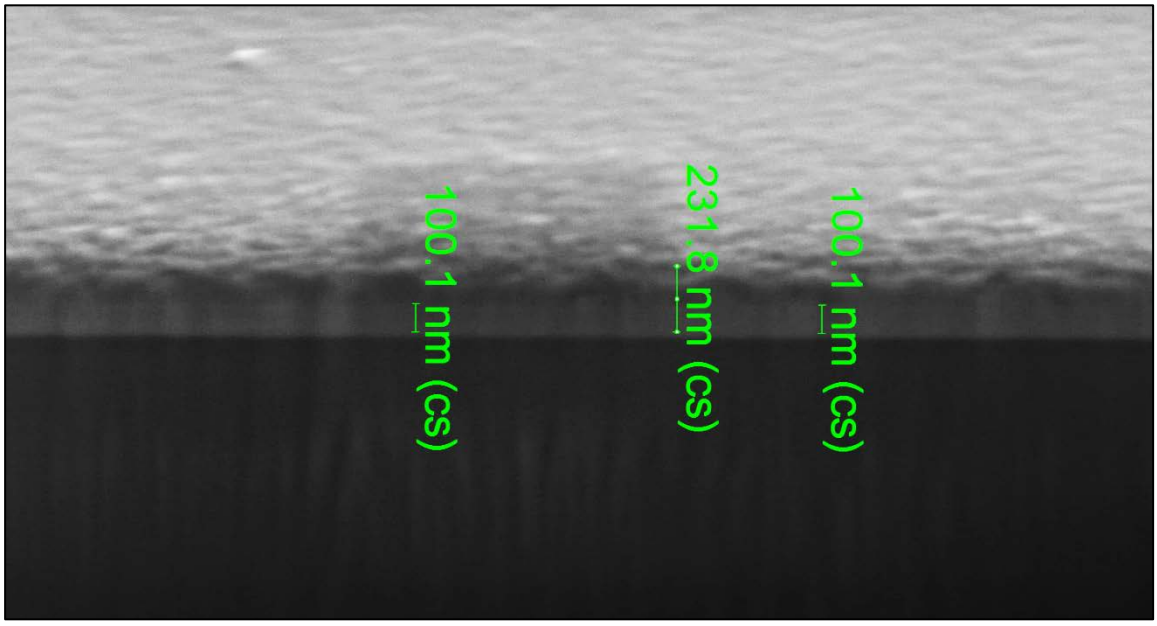

Figure 18: SEM image of sample A8 (Ti interlayer thickness of 100 ± 5 nm, total coating thickness of 232 ± 5 nm).

Clearly, the amount of flatware present inside the chamber during deposition has a significant influence on the deposition rate. The cycle with 240 parts in the chamber experienced a deposition rate that was greater than 3 times that of the cycle with 480 parts in the chamber. Since the consistency of coatings between cycles is of significant importance, the number of pieces of flatware coated in each cycle should remain constant. Figure 19 shows a comparison of the adhesion properties of samples A5 and A8 obtained from scratch testing.

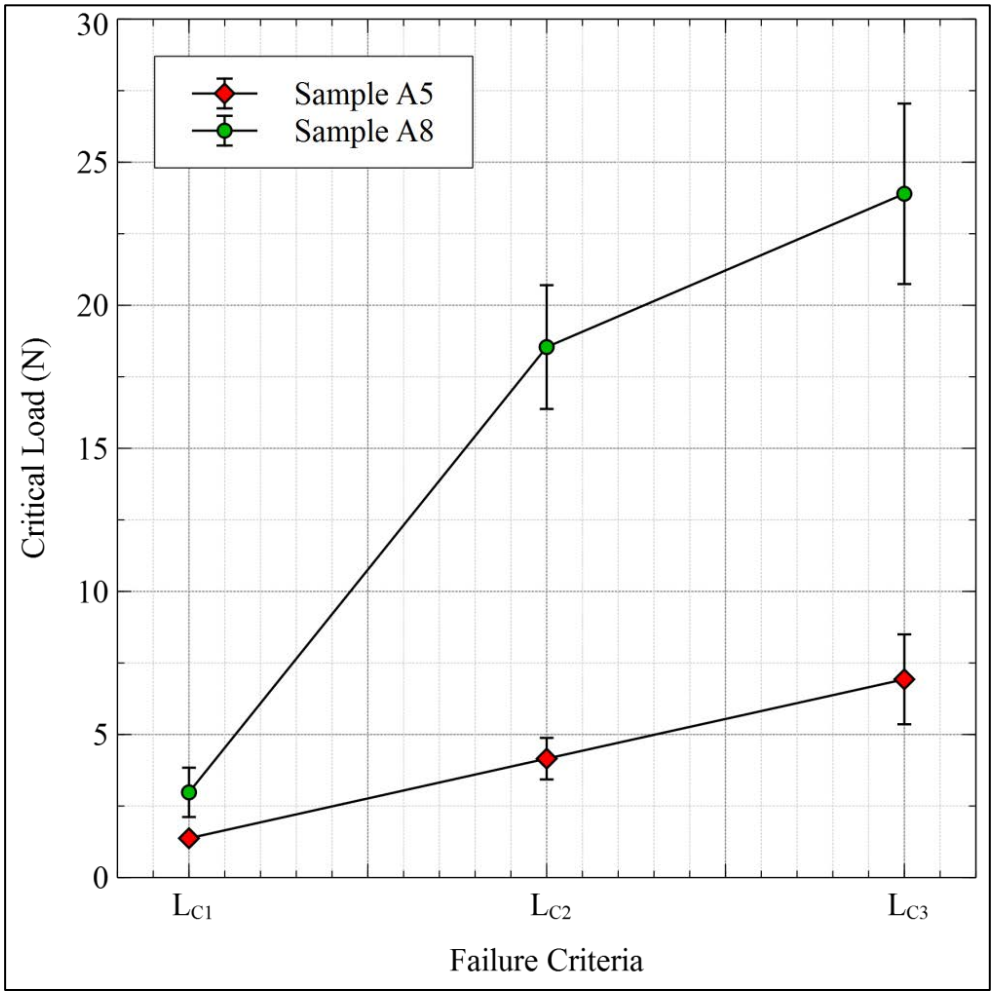

Figure 19: Adhesion results of samples A5 and A8 obtained from scratch testing.

Sample A5 had the worst adhesion properties of all of the samples that were scratch tested throughout the course of this research, likely due to the extremely thick Ti interlayer at approximately 360 nm (note: sample A2 had the worst adhesion of all of the samples, however, it showed immediate delamination after deposition and therefore could not be scratch tested). The Ti interlayer is very soft compared to both the steel substrate and the TiCN top layer and as a result of this, having too thick of a Ti interlayer will

cause the entire Ti/TiCN coating to deform very easily when a scratch is applied to the surface. Full delamination started to occur very early on when performing scratch tests on sample A5 which can be seen in Figure 20b.

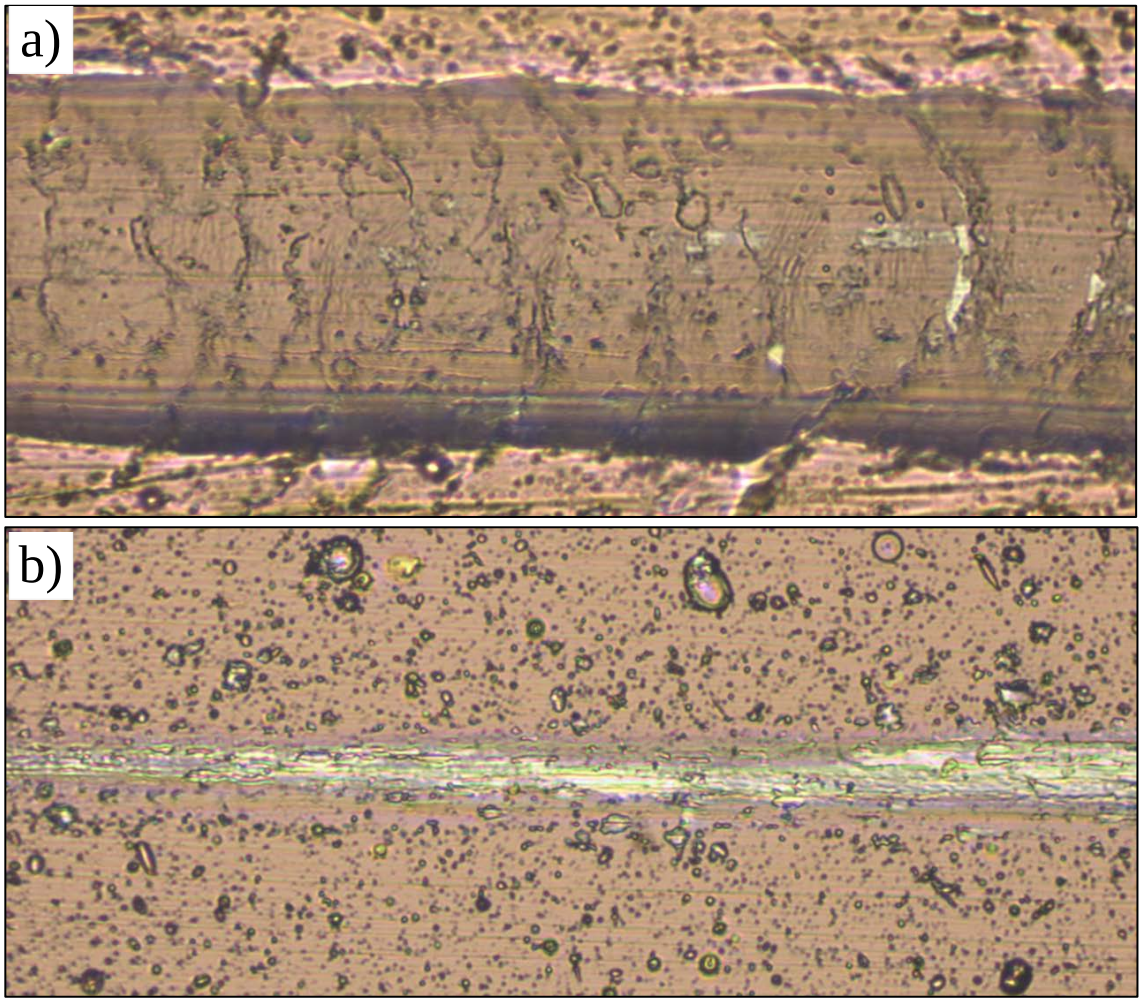

Figure 20: a) Scratch path on sample A8 which exhibits good adhesion, and b) scratch path on sample A5 which exhibits poor adhesion. Note the full delamination on sample A5 occurring at a very low applied load which is indicated by the narrow scratch width (both images were taken at 500x magnification).

Consistency Test for Deposition Rate and Adhesion

After finding such drastic differences in coating thicknesses between samples A5 and A8, it was necessary to see if these differences were in fact caused by the different numbers of parts inside the chamber and not by an unknown variable. Samples A10 and A11 were produced in consecutive cycles using identical deposition parameters (7 minute Ti interlayer, 13 minute TiCN top layer). Both samples had large forks as the substrates, which were supported on the upper level of the sample holding rack, and both cycles contained 320 parts inside the chamber during deposition. SEM images of the two coatings along with their thicknesses can be seen in Figure 21.

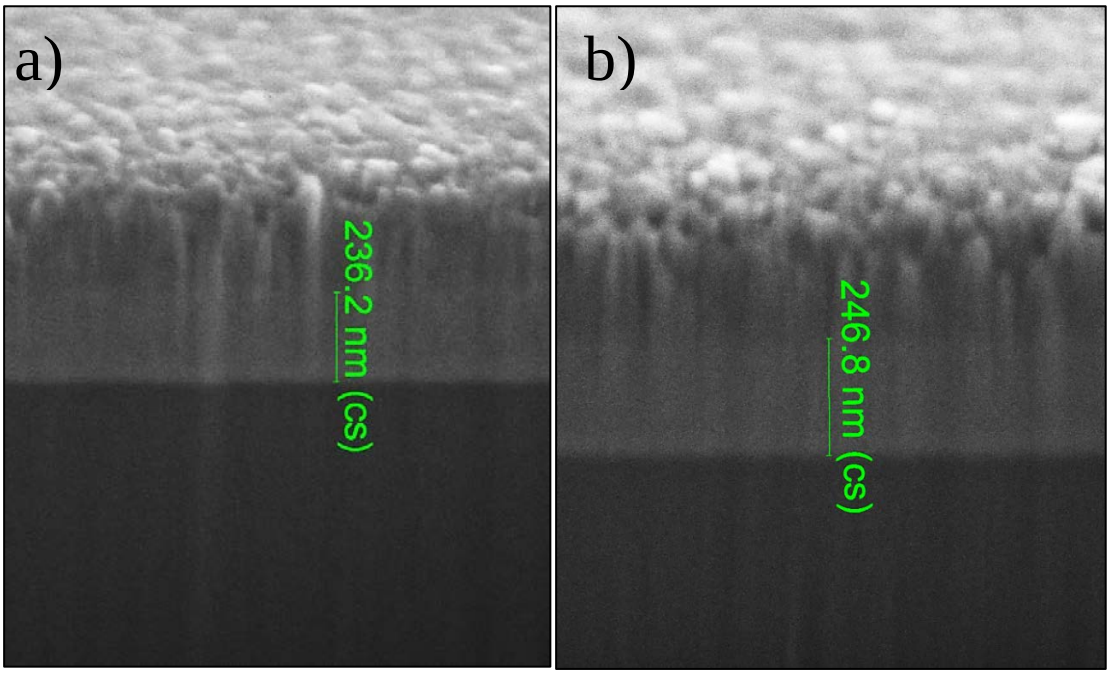

Figure 21: a) SEM image of sample A10 (Ti interlayer thickness of 236 ± 5 nm), and b) SEM image of sample A11 (Ti interlayer thickness of 247 ± 5 nm).

In both of these images, the contrast between the Ti interlayer and the TiCN top layer was quite difficult to observe, however, an interface can still be faintly seen. The two coatings appear to be nearly identical in terms of Ti interlayer thickness as well as total thickness which indicates that the system can in fact produce repeatable coatings if all deposition variables are kept constant between cycles. Furthermore, the adhesion properties of the two coatings are statistically similar, as can be seen in Figure 22.

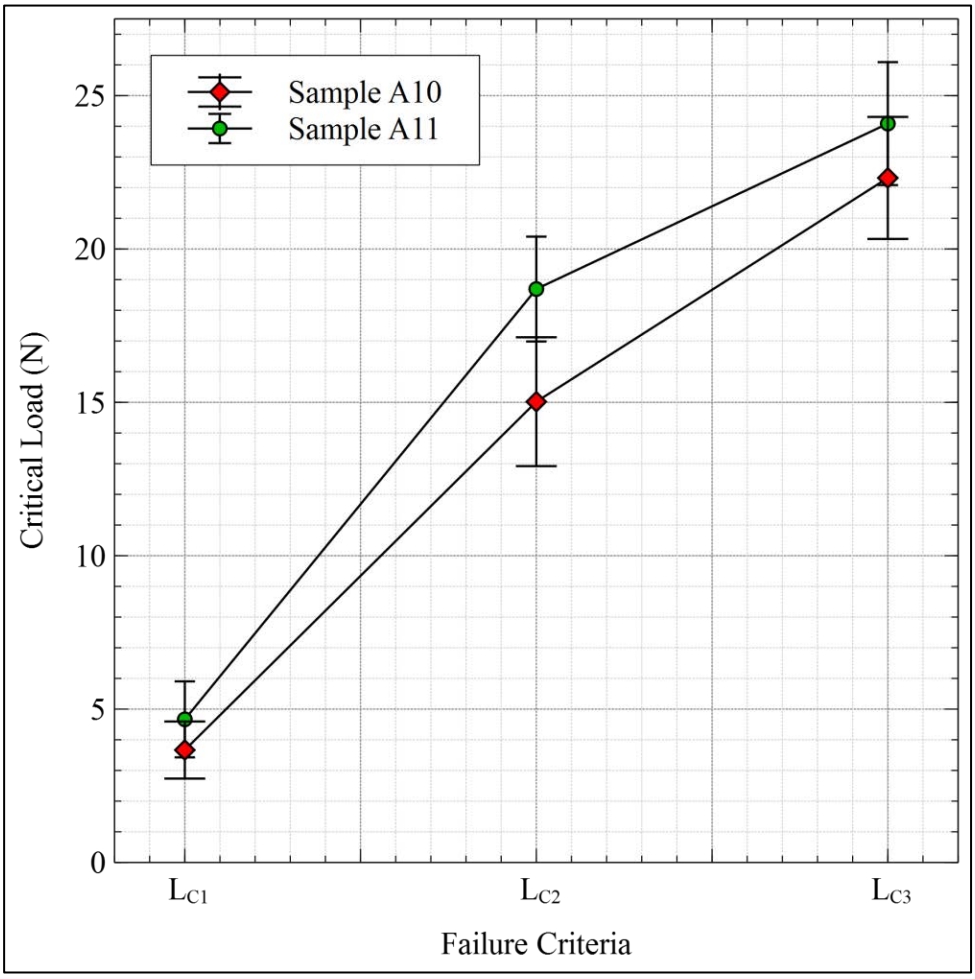

Figure 22: Adhesion results of samples A10 and A11 obtained from scratch testing.

Influence of New Ti Cathode Targets on Deposition Rate and Adhesion

As the titanium cathode targets are evaporated to deposit the coating during deposition, they will eventually become depleted and will need to be replaced. A new titanium target has the shape of a cylindrical puck measuring approximately 4 inches in diameter by 1 inch thick. A target is considered depleted when the evaporation process has left a well in the target close to 1 inch deep as can be seen in Figure 23.

Figure 23: New (left) versus depleted (right) titanium cathode targets.

Under a typical production schedule – while using the cathodic arc PVD system multiple times per day on a daily basis – the targets will go from new to depleted in approximately 2 to 3 months. An experiment was conducted to see if the deposition rate of the system would change when all 10 depleted titanium targets were changed to new

targets. As mentioned in the previous experiment, samples A10 and A11 were produced in consecutive cycles using identical deposition parameters, and the titanium targets that were used during those depositions were all nearing depletion. After completing those two cycles, all 10 of the titanium targets were replaced with brand new targets. Sample A12 was deposited in the first cycle after replacing all 10 targets using deposition parameters identical to samples A10 and A11 (i.e. 7 minute Ti interlayer, 13 minute TiCN top layer, using a large fork as the substrate, which was supported on the upper level of the sample holding rack, and containing 320 parts inside the chamber during deposition). An SEM image of the cross section of sample A12 can be seen in Figure 24.

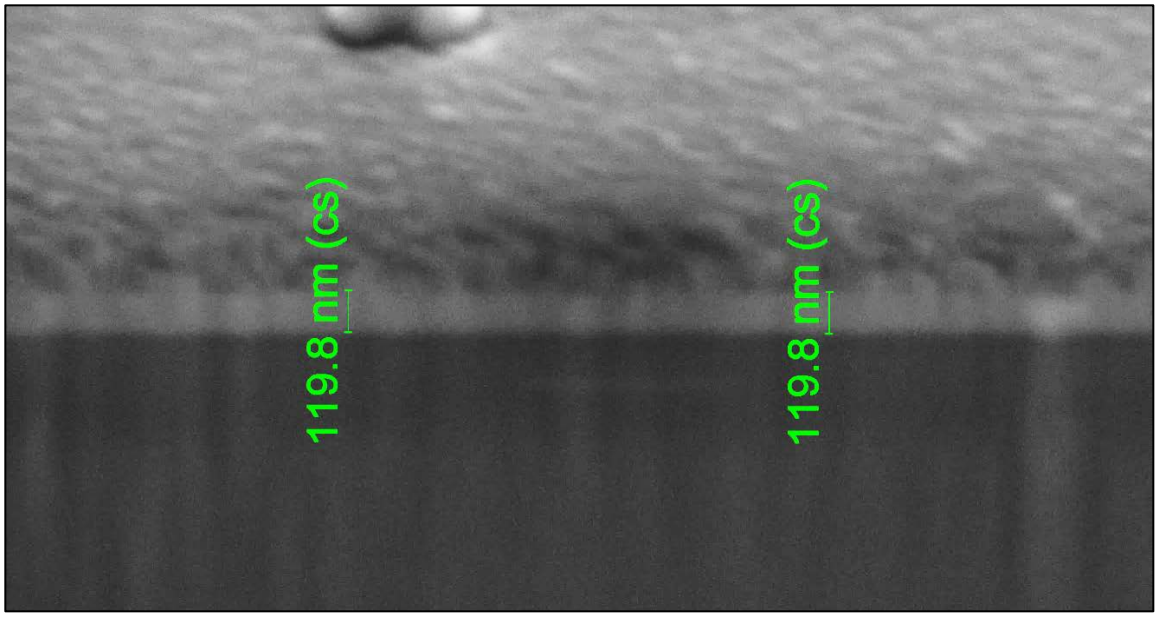

Figure 24: SEM image of sample A12 (Ti interlayer thickness of 120 ± 5 nm).

When comparing the SEM results of Figure 24 with those shown in Figure 21, it is clear that the deposition rate is significantly lower when using new titanium cathode

targets compared to using targets that have already been ‘burned-in’. Samples A10 and A11 have Ti interlayer thicknesses of approximately 240 nm, while sample A12 has a Ti interlayer thickness of only about 120 nm, indicating that there is a substantial (50%) decrease in the deposition rate when using 10 brand new targets.

Cathodic arc processes are highly dependent on the surface state of the cathode material. A pure metal like titanium will be much more easily evaporated by an electrical arc than a non-metallic layer such as titanium oxide or titanium nitride. If an electrical arc is ignited on a non-metallic cathode surface, the current per emission center, otherwise known as an arc spot, is much smaller than if it was ignited on a pure metallic surface, and it will not form a continuous arc erosion pattern on the surface of the cathode target during operation [13]. When the new targets were installed inside of the chamber, they likely had titanium oxide layers that had developed on their surfaces after being kept in storage for several months. This decreased the deposition rate of the system since the deposition rate is related to the size of the arc spot. Targets that have already been ‘burned-in’ do not experience this problem since the oxides on their surfaces have already been evaporated off via the electrical arcs, and the pure titanium underneath is not able to re-oxidize very easily since the targets are kept under vacuum. It is important to keep this in mind when routinely changing out depleted targets in the system; only one of the 10 targets should be changed at a time to minimize the change in deposition rate. After the new target has been ‘burned-in’, another depleted target can be changed out and so on.

Another option is to physically remove the oxide layer by sanding or grinding the surface of the new targets prior to installation so that the 'burn-in' period can be reduced. Interestingly enough, sample A12 had the best adhesion results of the three samples as can be seen in Figure 25. It should be noted that for sample A12, the critical load criterion L_{C3} was never reached within the maximum applied force range of 0 to 30N during the 5 scratches performed with the scratch tester, so it is indicated as >30 N in Figure 25.

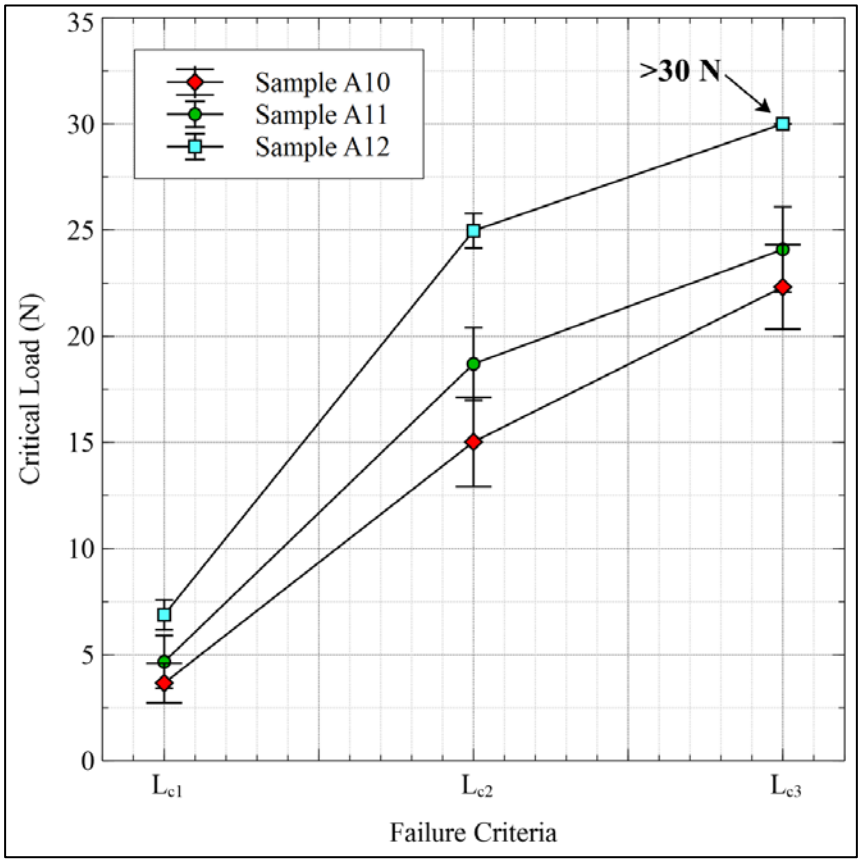

Figure 25: Adhesion results of samples A10, A11, and A12 obtained from scratch testing.

Sample A12 was also noticeably grainier in texture than all of the other samples produced in this research, likely due to the inconsistent evaporation state of the oxidized target surfaces. A texture comparison of sample A12 with a sample from a typical deposition cycle can be seen in Figure 26.

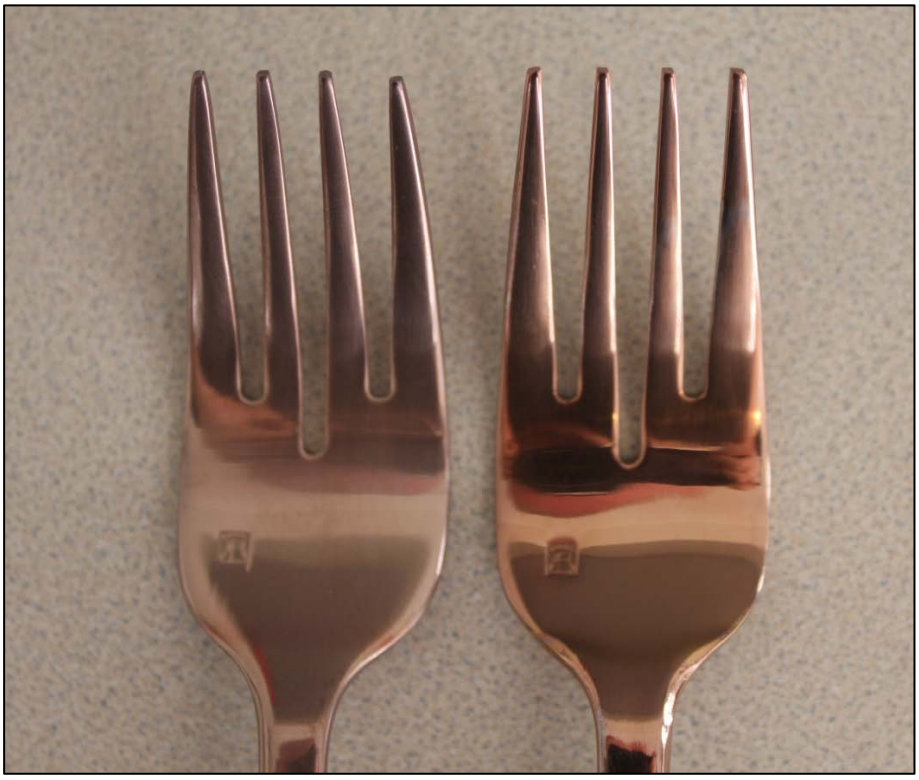

Figure 26: Texture comparison of sample A12 (left) with a sample from a typical deposition cycle (right). Notice the significant difference in reflection.

Deposition Rate and Adhesion vs. Utensil Size

Since it was found previously that the amount of substrate material inside of the chamber (i.e. the number of utensils inside of the chamber) had a significant effect on the deposition rate of the coating, an experiment was conducted to see if the size of the utensils being coated would also have an influence on the deposition rate. Two deposition cycles were performed consecutively using the same deposition parameters (5 minute Ti interlayer duration, 10 minute TiCN layer duration), however, the first cycle was loaded with 360 small salad forks (7 ¼ inches in length) and the second cycle was loaded with 360 large dinner forks (8 ½ inches in length). Sample A15 was a small salad fork taken from the first deposition cycle and sample A16 was a large dinner fork taken from the second deposition cycle. Based on the results of the test with the varying number of utensils inside the chamber, it was hypothesized that the smaller forks would receive a thicker coating than the larger forks using the same deposition parameters since there would be less substrate surface area to coat inside of the chamber. Figure 27 shows SEM images of the two coatings on silicon wafers that were loaded in each cycle.

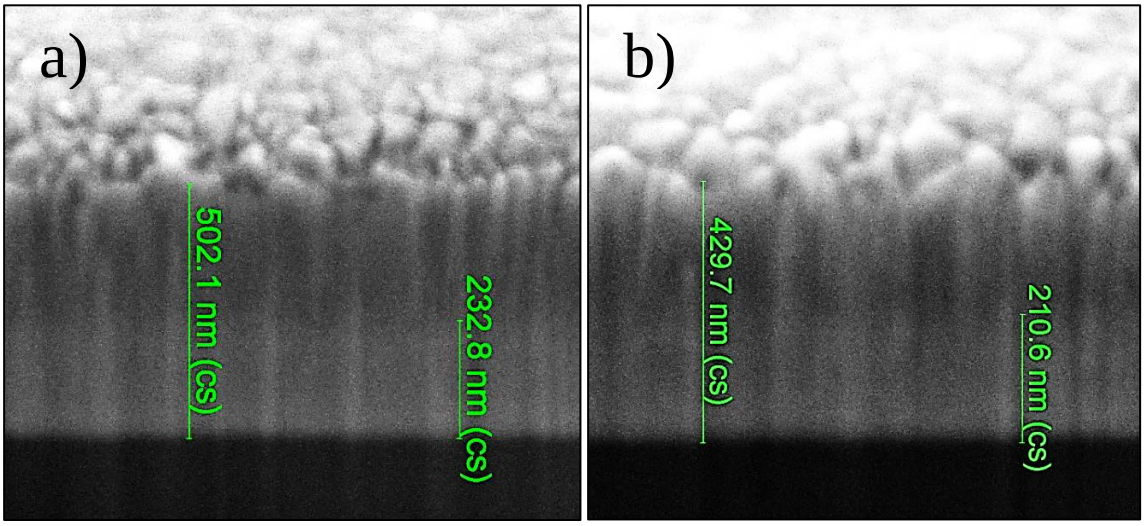

Figure 27: a) SEM image of sample A15 taken from the cycle with small salad forks, and b) SEM image of sample A16 taken from the cycle with large dinner forks.

The transition between the Ti interlayer and the TiCN top layer can be faintly made out in both SEM images, and they show that the coatings on the small salad forks (Ti interlayer thickness of 233 ± 5 nm, total coating thickness of 502 ± 5 nm) were indeed slightly thicker than the coatings on the large dinner forks (Ti interlayer thickness of 211 ± 5 nm, total coating thickness of 430 ± 5 nm). Figure 28 shows a comparison of the adhesion properties of samples A15 and A16 obtained from scratch testing. As was the case with sample A12, when scratch testing sample A15, the critical load criterion L_{C3} was never reached within the maximum applied force range of 0 to 30N, so it is indicated as >30 N in Figure 28.

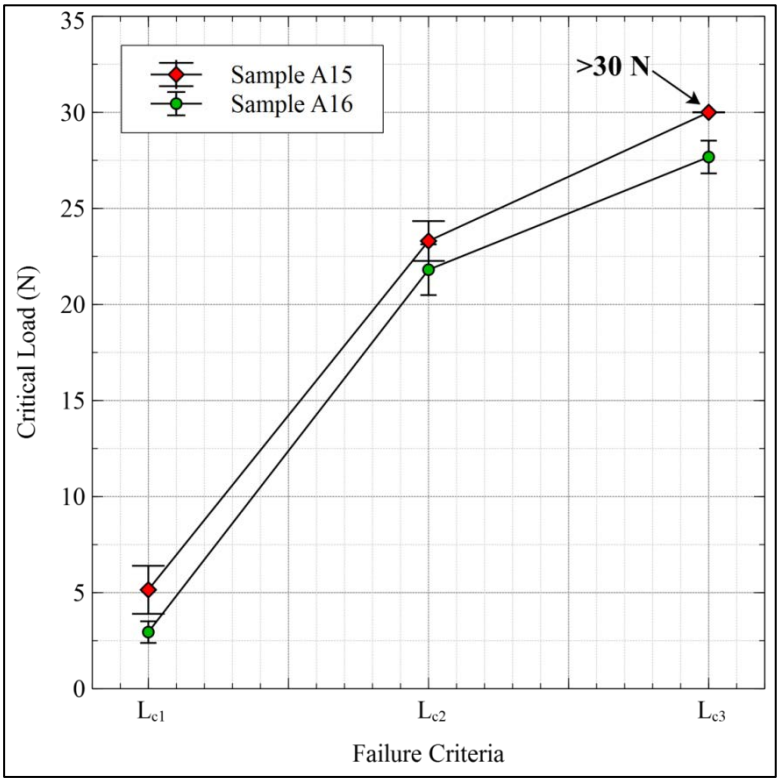

Figure 28: Adhesion results of samples A15 and A16 obtained from scratch testing.

In order to ensure that consistent and high quality coatings are being deposited when using the PVD system for the mass production of coated tableware, further testing should be done to determine the differences in deposition rates between all types of tableware utensils. Even though there is not a substantial difference in adhesion quality and film thickness between the salad fork and dinner fork cycles, this discrepancy may be more pronounced for drastically different items such as very small dessert forks and very large serving forks. After determining the differences in deposition rates between different items, the deposition duration should be appropriately adjusted to to keep the coatings consistent and predictable.

Deposition Rate and Adhesion vs. Utensil Mounting Location

During deposition, the utensils are held inside the chamber on steel racks as can be seen in Figure 29. The racks are mounted inside of the chamber on a rotating carousel base. As the base rotates, the individual racks also rotate so that all of the utensils pass directly in front of the titanium cathode targets for an equal amount of time. Half of the utensils are mounted on the upper level of the racks and the other half are mounted 9.5 inches below, on the lower level of the racks.

Figure 29: Mounting racks for coating utensils.

An experiment was performed to see if there was a difference in deposition rate and/or adhesion properties of the coatings between utensils mounted on either the upper or the lower levels of the racks. The two samples used for this experiment were prepared in the same deposition cycle with a 5 minute deposition of the Ti interlayer and a 10

minute deposition of the TiCN top layer. Silicon wafers were mounted on both the top and bottom levels of the rack, beside each utensil that would be used for adhesion testing. Sample A16 was a large dinner fork mounted on the top level of the rack and sample A17 was a large dinner fork mounted directly underneath A16 on the bottom level of the rack. SEM images of the two coatings can be seen in Figure 30.

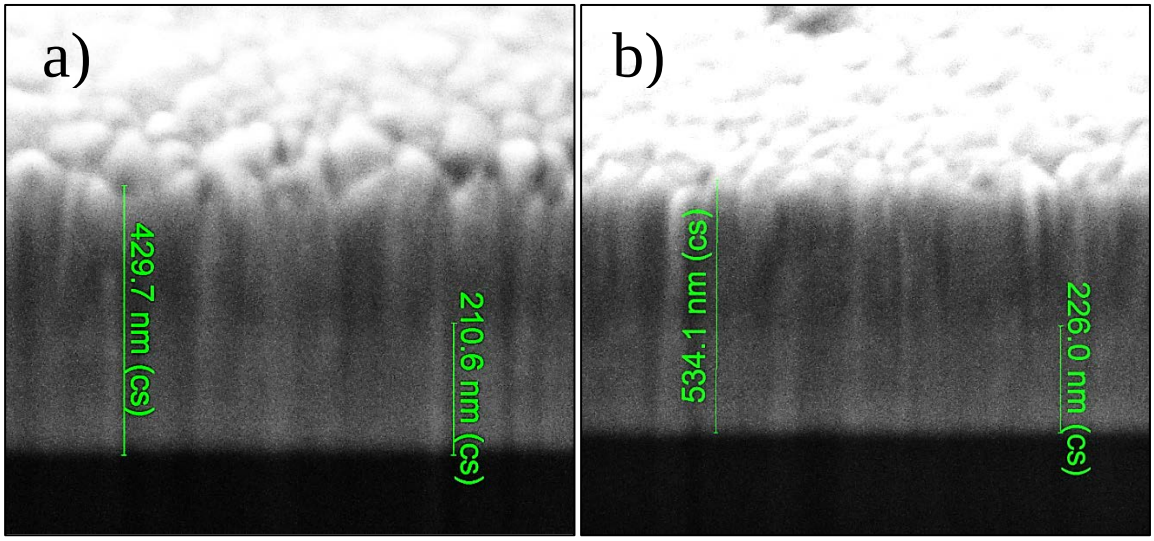

Figure 30: a) SEM image of sample A16 mounted on the upper rack level, and b) SEM image of sample A17 mounted on the lower rack level.

The transition between the Ti interlayer and the TiCN top layer can be faintly made out in both SEM images, and they show that the utensils mounted on the bottom level of the rack received a slightly thicker coating (Ti interlayer thickness of 226 ± 5 nm, total coating thickness of 534 ± 5 nm) than the utensils mounted on the top level of the rack (Ti interlayer thickness of 211 ± 5 nm, total coating thickness of 430 ± 5 nm). Figure 31 shows a comparison of the adhesion properties of samples A16 and A17

obtained from scratch testing. Again, when scratch testing sample A17, the critical load criterion L_{C3} was never reached within the maximum applied force range of 0 to 30N, so it is indicated as >30 N in Figure 31.

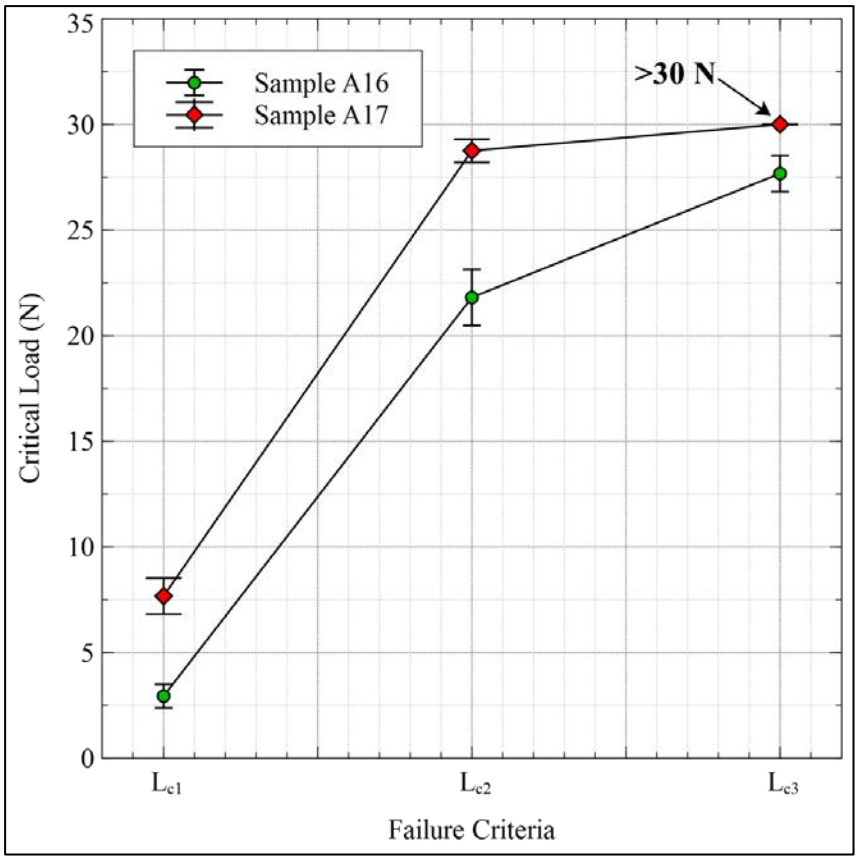

Figure 31: Adhesion results of samples A16 and A17 obtained from scratch testing.

It is quite interesting that there is such a pronounced difference in adhesion quality between these two samples considering that they were the only two samples in this entire research that were created in the same deposition cycle. This indicates that the utensil mounting location inside of the chamber has a significant influence on the adhesion quality of the deposited coating.

Although the Ti layer of the sample on the bottom rack level is only about 7% thicker than that of the sample on the top rack level, the TiCN layer of the sample on the bottom appears to be approximately 40% thicker. It has also been routinely observed that when depositing TiCN coatings using this PVD system, the utensils mounted on the bottom rack level have a slightly more violet colour to them after deposition than the utensils on the top rack level. This suggests that the carbon content is higher in the films of the utensils coated near the bottom of the chamber. Furthermore, it has been observed that when an arc occasionally malfunctions, usually by welding the anode pin to the surface of the cathode target upon contact, the utensils that are directly in a horizontal line of sight with the malfunctioning arc end up having a more violet colour than they normally would, again suggesting that the carbon content of the film is higher. It appears that the colour of the deposited films, and thus their carbon content, is dependent on the number of active arcs directly in a horizontal line of sight with the utensil being coated. It is likely the case then that the two rack levels used in this research for mounting the utensils (i.e. upper and lower rack position as can be seen in Figure 29) have slightly different exposure levels to the configuration of the 10 arcs located on the walls of the deposition chamber since they result in slightly different film colours and thicknesses. To minimize the effect of this, new racks should be designed that have taken into account the configuration of the arcs on the chamber walls, and the two mounting levels should be selected so as to have equal exposure and lines of sight with all 10 arcs.

Adhesion vs. Ti Interlayer Thickness

This final section aims to compare the Ti interlayer thicknesses of all of the samples prepared throughout this entire research along with their associated scratch test results to see if there is conclusive evidence to suggest an ideal Ti interlayer thickness to maximize the adhesion strength of the Ti/TiCN coating. Figure 32 shows a comparison of the critical loads obtained from scratch testing for all of the samples *versus* their Ti interlayer thicknesses. All of the raw data that was collected during this research, which is presented in Figure 32, can be found in Table 2 in the appendix section.

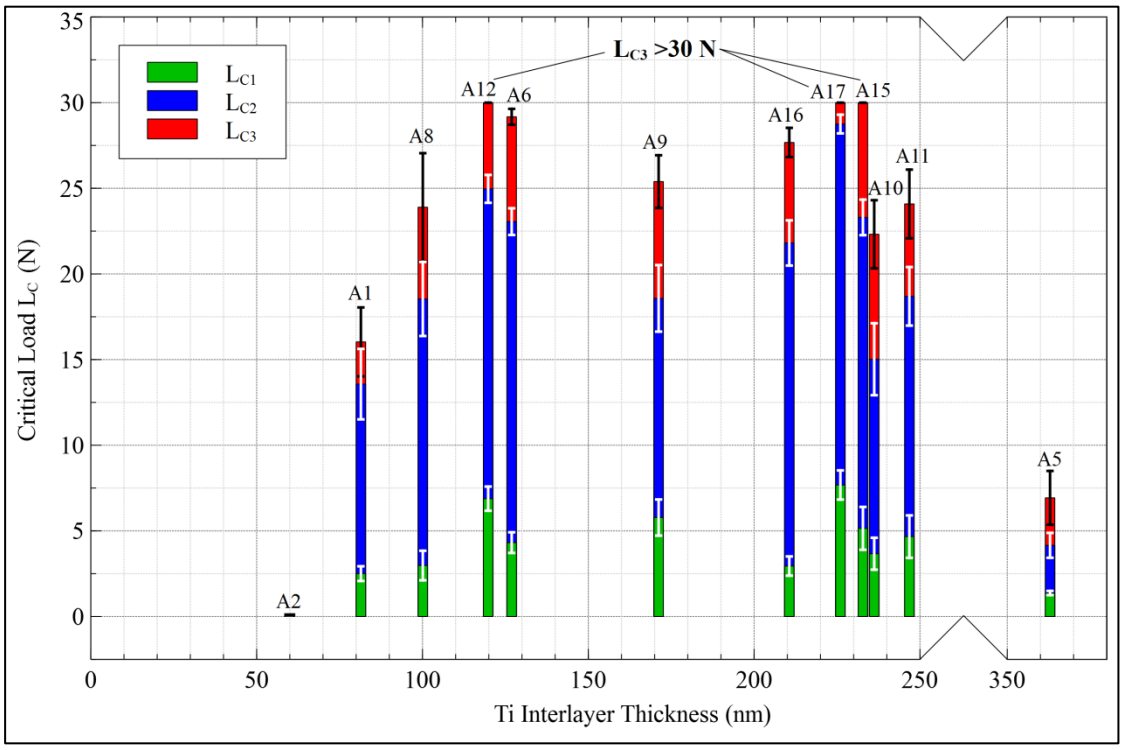

Figure 32: Critical loads of all samples obtained from scratch testing plotted against their Ti interlayer thicknesses.

As can be seen in Figure 32, the samples that exhibited the best adhesion properties were invariably contained in the thickness range of 120 to 233 nm. This is consistent with the findings of [6], [20], [21], where Ti interlayers in this range produced the best adhesion results for TiN coatings on stainless steel. Straying too far outside of this range clearly results in very poor adhesion of the TiCN coating as indicated by Samples A2 and A5 which had Ti interlayer thicknesses of 63 nm and 360 nm, respectively. This data is fairly conclusive, and to ensure good adhesion of TiCN coatings on stainless steel, a titanium interlayer between 120 and 233 nm should be deposited onto the substrate before depositing the TiCN layer.

Conclusions & Future Outlook

In this research, TiCN thin films were deposited on stainless steel substrates using a cathodic arc PVD system. Many parameters and conditions of the PVD system were varied, which had an influence on the deposition rate of the thin films, including the deposition rate of the Ti interlayer between the steel substrate and TiCN layer. The thickness of the Ti interlayer is an important factor in achieving good adhesion of the entire film, so determining how the deposition rate of the system is influenced by other factors is necessary for producing consistently high quality TiCN coatings.

The deposition rate of the system was initially found to be 28 ± 2 nm per minute. This deposition rate was found by depositing three TiCN thin films with different Ti interlayer deposition durations and averaging the deposition rates. The calculated deposition rate can only be used as a baseline value for the system however, since it assumes that (a) there are 360 teaspoons inside of the deposition chamber, (b) the Ti cathode targets are at the middle of their useful lives, and (c) the thickness is measured from a teaspoon from the top level of the mounting racks. Changing any of these conditions has a significant effect on the deposition rate of the system. Decreasing the number of utensils in the chamber will increase the thickness of the coatings on the remaining utensils, using larger utensils such as serving spoons will decrease the thickness of the coatings, using new Ti cathode targets that have not been ‘burned-in’ will

decrease the deposition rate of the system, and measuring samples that are mounted in the chamber on the lower level of the mounting rack will yield thicker coatings than samples mounted on the upper rack level.

It was found that TiCN samples which had Ti interlayer thicknesses between 120 and 233 nm exhibited the best adhesion properties. This is consistent with literature on TiN coatings that suggest Ti interlayers in the range of 100 to 300 nm for optimal adhesion. Regardless of the changes to the deposition conditions inside of the PVD chamber, the Ti interlayer thickness should always stay in this range for TiCN coatings. This can be achieved by adjusting the deposition duration accordingly.

Further research should be done to fully characterize the deposition rates for every size and type of utensil so that identical coatings can be deposited on each one. Research into non-arbitrary mounting rack positions should also be performed so that coatings which are deposited on utensils at different mounting heights inside of the chamber have the same thickness. To further minimize the changes in deposition rate between cycles, a single quantity of utensils (i.e., 360) should be used for all deposition cycles, and titanium cathode targets should only be replaced one at a time, waiting until the new target has gone through a sufficient ‘burn-in’ period before replacing the next one.

This research could further benefit from having more samples with Ti interlayer thicknesses in the ranges of 0 to 50 nm and 250 to 350+ nm. This would allow for more

data points to be collected outside of the optimal Ti interlayer thickness range, providing a stronger justification for the importance of staying within this range for optimizing adhesion. One reason that this was not done was that the thicknesses of the Ti interlayers were not known until SEM was performed on the samples, which was often weeks after deposition. Since the commercial PVD system was being used on daily basis for production purposes during this interim period, the depletion levels of the cathode targets were always different between sample sets, and trying to predict an accurate deposition duration that would produce a desired film thickness was not feasible. Accurately tracking the usage of each cathode target during daily use of the PVD system while maintaining a documented target replacement schedule is highly recommended to keep the deposition rate of the system and the film thicknesses predictable and reproducible.

Overall, this research was very useful in understanding many of the factors that can influence the deposition process of large scale commercial cathodic arc PVD coatings. Academic research on thin films and deposition processes is often done in highly controlled and reproducible environments which has led to an excellent understanding of the underlying material physics of thin film technology, but it often misses the many problems inherent in large scale commercial deposition processes where many different objects are being coated simultaneously. As hard PVD coatings become increasingly used in improving the quality and appearance of consumer products, it is important not to overlook such issues.

References

[1] D. M. Mattox, “Handbook of Physical Vapor Deposition (PVD) Processing,” 2nd ed., Elsevier Inc., 2010, pp. 387–388.

[2] E. Santecchia, A. M. S. Hamouda, F. Musharavati, E. Zalnezhad, M. Cabibbo, and S. Spigarelli, “Wear resistance investigation of titanium nitride-based coatings,” *Ceram. Int.*, vol. 41, no. 9, pp. 10349–10379, Nov. 2015.

[3] S. Zhang and W. Zhu, “TiN coating of tool steels: a review,” *J. Mater. Process. Technol.*, vol. 39, no. 1–2, pp. 165–177, Oct. 1993.

[4] X. Liu, Y. Z. LU, and R. G. Gordon, “Improved Conformality of CVD Titanium Nitride Films,” *MRS Proc.*, vol. 555, p. 135, Jan. 1998.

[5] Y. Sun, “A study of TiN- and TiCN-based coatings on Ti and Ti6Al4V alloys,” University Of Wollongong, 2014.

[6] R. L. Boxman, D. M. Sanders, and P. J. Martin, “Handbook of Vacuum Arc Science and Technology: Fundamentals and Applications,” 1st ed., Noyes Publications, 1995, p. 474.

[7] H. Randhawa, “Cathodic Arc Plasma Deposition of TiC and TiCxN1-x Films,” *Thin Solid Films*, vol. 153, pp. 209–218, 1987.

[8] Aerospace Specification Metals Inc., “AISI Type 304 Stainless Steel.” [Online]. Available: http://asm.matweb.com/search/SpecificMaterial.asp?bassnum=mq304a. [Accessed: 09-Apr-2017].

[9] Y. Y. Guu, J. F. Lin, and C.-F. Ai, “The Tribological Characteristics of Titanium Nitride Coatings Part I. Coating Thickness Effects,” *Wear*, vol. 194, pp. 12–21, 1996.

[10] D. Dowson, C. M. Taylor, and M. Godet, “Mechanics of Coatings,” 1st ed., Elsevier Inc., 1990, p. 411.

[11] PVD Coatings, “FAQ.” [Online]. Available: http://www.pvdcoatings.net/faq#q4. [Accessed: 09-Apr-2017].

[12] D. M. Mattox, “Handbook of Physical Vapor Deposition (PVD) Processing,” 2nd ed., Elsevier Inc., 2010, pp. 287–288.

[13] A. Anders, “Cathodic Arc Plasma Deposition,” *Vac. Technol. Coat.*, vol. 3, no. 7–8, 2002.

[14] D. M. Mattox, “Handbook of Physical Vapor Deposition (PVD) Processing,” 2nd ed., Elsevier Inc., 2010, p. 295.

[15] W. Gissler and H. A. Jehn, Eds., “Advanced Techniques for Surface Engineering,” vol. 1, Dordrecht: Springer Netherlands, 1992, p. 44.

[16] Enparticles Diffusion Pump Oil, “Diffusion Pump Working Principle.” [Online]. Available: http://diffusionpumpoil.com/diffusion-pump-working-principle/. [Accessed: 05-Mar-2017].

[17] Enparticles Diffusion Pump Oil, “ECO-704 Silicone Diffusion Pump Oil.” [Online]. Available: https://diffusionpumpoil.com/product/eco-704-silicone-diffusion-pump-oil/. [Accessed: 05-May-2017].

[18] D. M. Mattox, “Handbook of Physical Vapor Deposition (PVD) Processing,” 2nd ed., Elsevier Inc., 2010, p. 291.

[19] “Cathodic arc deposition,” *Wikiwand*. [Online]. Available: http://www.wikiwand.com/en/Cathodic_arc_deposition.

[20] J. R. Yepes, J. M. G. Carmona, A. R. Muñoz, E. R. Parra, and F. S. Osorio, “Mechanical, and Tribological Properties of Ti/TiN Bilayers: The Dependence of Interlayer Thickness,” *Dyna*, vol. 80, no. 178, pp. 115–122, 2013.

[21] W. Gissler and H. A. Jehn, Eds., “Advanced Techniques for Surface Engineering,” vol. 1, Dordrecht: Springer Netherlands, 1992, p. 43.

[22] S. J. Bull *et al.*, “The influence of titanium interlayers on the adhesion of titanium nitride coatings obtained by plasma-assisted chemical vapour deposition,” *Mater. Sci. Eng. A*, vol. 139, no. C, pp. 71–78, 1991.

[23] D. M. Mattox, “Handbook of Physical Vapor Deposition (PVD) Processing,” 2nd ed., Elsevier Inc., 2010, p. 521.

[24] R. L. Boxman, D. M. Sanders, and P. J. Martin, “Handbook of Vacuum Arc Science and Technology: Fundamentals and Applications,” 1st ed., Noyes Publications, 1995, p. 385.

[25] S. A. Lyda, “Decorative and Protective TiN Coatings on 304 Stainless Steel Using Cathodic Arc PVD,” McMaster University, 2016.

[26] A. Brown, S. A. Lyda, J. Wojcik, and P. Mascher, “Application of Titanium Nitride Coatings on Stainless Steel Tableware for Decorative and Protective Purposes,” in *Society of Vacuum Coaters 59th Annual Technical Conference Procedings*, 2016.

[27] FEI Company, “An Introduction to Electron Microscopy: Focused Ion Beam Systems and DualBeam™ Systems.” [Online]. Available: https://www.fei.com/introduction-to-electron-microscopy/fib/. [Accessed: 07-Mar-2017].

[28] T. Nsongo and M. Gillet, “Adhesion characterization of titanium and titanium nitride thin coatings on metals using the scratch test,” *Int. J. Adhes. Adhes.*, vol. 15, no. 3, pp. 191–196, Jul. 1995.

Appendix

Table 2: Scratch test results and SEM thickness measurements for all samples.

Scratch Test	L_{C1} (mN)	L_{C2} (mN)	L_{C3} (mN)
Sample A1 - Scratch 1	1177.23	17448.73	21923.50
Sample A1 - Scratch 2	1744.22	14910.68	16313.16
Sample A1 - Scratch 3	2012.03	11166.31	11166.31
Sample A1 - Scratch 4	5060.09	18441.12	19953.06
Sample A1 - Scratch 5	2524.34	5861.41	10803.44
Average	2503.58	13565.65	16031.89
Standard Deviation	1350.08	4599.34	4498.36
Standard Error	603.78	2056.89	2011.73
Ti-Interlayer Thickness of Sample A1 = 83 ± 5 nm			
No scratch testing was performed on Sample A2 due to premature delamination			
Ti-Interlayer Thickness of Sample A2 = 63 ± 5 nm			
Sample A5 - Scratch 1	1275.88	5243.18	8921.57
Sample A5 - Scratch 2	1009.64	2958.22	3851.04
Sample A5 - Scratch 3	1699.48	1699.48	1699.48
Sample A5 - Scratch 4	1199.97	4649.58	9373.36
Sample A5 - Scratch 5	1677.63	6225.41	10792.64
Average	1372.52	4155.17	6927.62
Standard Deviation	272.32	1623.40	3512.68
Standard Error	121.78	726.01	1570.92
Ti-Interlayer Thickness of Sample A5 = 360 ± 5 nm			
Sample A6 - Scratch 1	4837.60	21409.66	29312.73
Sample A6 - Scratch 2	4021.09	21204.63	27596.14
Sample A6 - Scratch 3	5717.64	22442.32	28845.92
Sample A6 - Scratch 4	4183.22	24745.12	28270.40

Sample A6 - Scratch 5	2807.23	25471.50	29587.56
Average	4313.36	23054.65	28722.55
Standard Deviation	961.00	1743.70	719.03
Standard Error	429.77	779.80	321.56
Ti-Interlayer Thickness of Sample A6 = 127 ± 5 nm			
Sample A8 - Scratch 1	1242.82	9813.68	9813.68
Sample A8 - Scratch 2	1912.63	19744.62	28105.33
Sample A8 - Scratch 3	1410.00	17768.03	26916.07
Sample A8 - Scratch 4	6263.48	24172.79	27178.40
Sample A8 - Scratch 5	4057.03	21193.96	27461.68
Average	2977.19	18538.62	23895.03
Standard Deviation	1926.82	4836.68	7051.80
Standard Error	861.70	2163.03	3153.66
Ti-Interlayer Thickness of Sample A8 = 100 ± 5 nm			
Sample A9 - Scratch 1	6941.17	21408.65	26758.61
Sample A9 - Scratch 2	7997.22	17588.31	26595.28
Sample A9 - Scratch 3	3147.32	10493.44	19700.05
Sample A9 - Scratch 4	2728.61	21105.99	23893.64
Sample A9 - Scratch 5	8077.81	22270.23	29374.61
Average	5778.43	18573.32	25264.44
Standard Deviation	2357.38	4344.55	3278.37
Standard Error	1054.25	1942.94	1466.13
Ti-Interlayer Thickness of Sample A9 = 171 ± 5 nm			
Sample A10 - Scratch 1	7259.43	20037.23	24682.83
Sample A10 - Scratch 2	3080.49	7597.11	13768.16
Sample A10 - Scratch 3	4309.80	20145.44	24355.06
Sample A10 - Scratch 4	2643.24	13569.40	26322.15
Sample A10 - Scratch 5	1033.62	13753.09	22447.54
Average	3665.32	15020.45	22315.15
Standard Deviation	2080.65	4695.77	4447.29
Standard Error	930.49	2100.01	1988.89

Ti-Interlayer Thickness of Sample A10 = 236 ± 5 nm			
Sample A11 - Scratch 1	6757.03	22749.87	25351.55
Sample A11 - Scratch 2	6658.41	21974.77	26313.99
Sample A11 - Scratch 3	2013.86	12062.01	15190.27
Sample A11 - Scratch 4	7258.97	17455.70	27050.13
Sample A11 - Scratch 5	637.14	19222.19	26523.91
Average	4665.08	18692.91	24085.97
Standard Deviation	2768.80	3821.24	4481.72
Standard Error	1238.24	1708.91	2004.29
Ti-Interlayer Thickness of Sample A11 = 247 ± 5 nm			
Sample A12 - Scratch 1	6156.15	26015.05	>30000
Sample A12 - Scratch 2	8144.79	21582.69	>30000
Sample A12 - Scratch 3	7494.80	26903.24	>30000
Sample A12 - Scratch 4	4141.26	25471.13	>30000
Sample A12 - Scratch 5	8461.36	24858.94	>30000
Average	6879.67	24966.21	N/A
Standard Deviation	1581.33	1820.26	N/A
Standard Error	707.19	814.05	N/A
Ti-Interlayer Thickness of Sample A12 = 120 ± 5 nm			
Sample A15 - Scratch 1	3908.78	20811.58	>30000
Sample A15 - Scratch 2	4622.35	23617.04	>30000
Sample A15 - Scratch 3	901.74	22827.96	>30000
Sample A15 - Scratch 4	7361.06	21725.01	>30000
Sample A15 - Scratch 5	8938.48	27529.63	>30000
Average	5146.48	23302.24	N/A
Standard Deviation	2796.71	2318.88	N/A
Standard Error	1250.73	1037.03	N/A
Ti-Interlayer Thickness of Sample A15 = 233 ± 5 nm			
Sample A16 - Scratch 1	3013.10	23166.76	25884.67
Sample A16 - Scratch 2	1268.85	16786.70	26087.66

Sample A16 - Scratch 3	2813.34	25419.13	26395.57
Sample A16 - Scratch 4	5147.63	20513.86	29283.34
Sample A16 - Scratch 5	2485.74	23153.20	28968.77
Average	2945.73	21807.93	27324.00
Standard Deviation	1256.50	2952.43	1483.68
Standard Error	561.92	1320.37	663.52
Ti-Interlayer Thickness of Sample A16 = 211 ± 5 nm			
Sample A17 - Scratch 1	10741.06	28119.27	>30000
Sample A17 - Scratch 2	7787.13	28859.12	>30000
Sample A17 - Scratch 3	6589.58	26775.42	>30000
Sample A17 - Scratch 4	8280.89	29734.37	>30000
Sample A17 - Scratch 5	4994.96	29422.88	>30000
Average	7678.72	28582.21	N/A
Standard Deviation	1904.79	1057.33	N/A
Standard Error	851.85	472.85	N/A
Ti-Interlayer Thickness of Sample A17 = 226 ± 5 nm			